Double Machine Learning for Dynamic Panel Data: Inference in High-Dimensional Time Series

Lucas Sneller

January 26, 2026

Abstract

Standard double machine learning (DML) theory is developed for i.i.d. data and does not directly fit dynamic panels with serial dependence. I develop a DML approach for inference on a treatment/policy coefficient in a partially linear dynamic panel with high-dimensional controls, where nuisance components are estimated using machine learning. I propose blocked-time cross-fitting with an optional time buffer to respect the panel's temporal structure, combined with a Neyman-orthogonal partialling-out score and a feasible unit-clustered variance estimator. Under cross-sectional independence and weak within-unit dependence, and under standard product-rate conditions for nuisance learning, I establish that the resulting estimator is asymptotically normal with $\sqrt{N}$ scaling and provide a feasible clustered variance estimator. Monte Carlo experiments illustrate when orthogonalization and cross-fitting improve bias and coverage relative to naive post-ML approaches, and where short-panel limitations can remain material.

Keywords: Dynamic panel data; debiased ML; cross-fitting; high-dimensional covariates; structural inference; Lasso; random forests.
JEL: C14; C23; C52.

1 Introduction

Dynamic panel data models are foundational in empirical economics and finance. They capture persistence, adjustment dynamics, and the intertemporal propagation of shocks, while leveraging repeated observations to control for unobserved heterogeneity. At the same time, modern empirical designs increasingly rely on rich covariate sets (text, transactions, networks, high-frequency aggregates, or flexible transformations) to reduce confounding and to improve predictive content. These trends create an inference problem: classical dynamic panel estimators were designed for low-dimensional nuisance structure, while modern machine learning (ML) methods introduce regularization and overfitting biases that invalidate naive post-ML inference.

This paper develops a double/debiased machine learning (DML) approach to inference in a *partially linear dynamic panel* model with high-dimensional controls. We focus on a setting in which the object of interest is a *dynamic target parameter*—a coefficient on a policy/treatment regressor

in the presence of lagged outcomes and flexible controls—while nuisance components (conditional expectations and/or nonlinear functions of covariates) are estimated with ML. The core idea is to combine (i) orthogonal (Neyman-orthogonal) score construction and (ii) sample splitting with cross-fitting to eliminate first-order sensitivity of the target estimator to nuisance estimation error. This is in the spirit of Chernozhukov et al. [2018], but adapted to panel/time-series dependence and dynamic specifications.

This paper provides a practically implementable framework that addresses the specific challenges of dynamic panels: we construct an orthogonal score for the target parameter that accounts for lagged outcomes and fixed effects, we design a cross-fitting scheme that respects serial dependence through blocked-time folds, and we establish asymptotic normality with feasible cluster-robust variance estimation under weak dependence conditions.

1.1 Motivation: dynamics, high dimensionality, and invalid naive inference

To fix ideas, consider a panel $\{(Y_{it}, D_{it}, X_{it}) : i = 1, \ldots, N;\ t = 1, \ldots, T\}$ with unit effects. A natural empirical specification is

$$Y_{it} = \rho_0 Y_{i,t-1} + \theta_0 D_{it} + g_0(X_{it}) + \alpha_i + U_{it}, \tag{1}$$

As a concrete illustration, consider estimating how bank lending responds to monetary policy changes in a panel of banks over time. Here, Y_{it} is loan growth at bank i in period t, D_{it} is a measure of monetary policy stance (e.g., the federal funds rate or a policy shock), and X_{it} includes high-dimensional controls such as bank balance sheet characteristics, regulatory filings, earnings call transcripts, and macroeconomic indicators. Dynamics are essential because loan growth exhibits persistence (banks adjust lending gradually); the influence of past policy can operate through the dynamic structure and through flexible controls for policy histories, even though the target coefficient remains on contemporaneous D_{it}. The target parameter θ_0 captures the contemporaneous effect of policy stance on loan growth within a dynamic model; longer-horizon responses also depend on the persistence parameter ρ_0. In the general model (1), D_{it} is a treatment/policy variable, X_{it} is a high-dimensional vector of controls, $g_0(\cdot)$ is an unknown (potentially nonlinear) function, α_i is an unobserved time-invariant effect, and U_{it} is an idiosyncratic disturbance. Even in low dimensions, dynamic panels pose well-known complications: fixed effects interact with lagged outcomes to produce finite-T bias (Nickell [1981]), motivating specialized estimators and specification tests (Arellano and Bond [1991]). In high dimensions, the situation worsens: if researchers use ML to estimate g_0 (or associated nuisance regressions) and then "plug in" those estimates into a second-stage regression for θ_0, regularization bias and overfitting can dominate the sampling distribution. As emphasized in the DML literature, naive ML-based inference is generally invalid because nuisance estimation errors enter the target estimator at first order unless orthogonalization and sample splitting are used (Chernozhukov et al. [2018]).

1.2 Contributions

This paper makes three main contributions to the literature on inference in dynamic panels with high-dimensional controls. (i) **Dependence-aware cross-fitting for dynamic panels.** We provide a blocked-time cross-fitting scheme with an optional buffer that respects serial dependence in panel data by holding out contiguous blocks of time periods across all units. This fold construction separates training and test sets in time, reducing overfitting bias while remaining compatible with weak serial dependence under the mixing conditions. (ii) **Orthogonal score for dynamic target parameters.** We construct a Neyman-orthogonal score for the target parameter θ_0 in a partially linear dynamic panel model, where nuisance objects include conditional expectations of (Y_{it}, D_{it}) given covariates and lagged outcomes. The orthogonalization ensures that nuisance estimation error affects the target estimator only at second order, enabling valid inference even when nuisance functions are estimated with machine learning methods such as Lasso or random forests. (iii) **Feasible inference under weak dependence.** We establish high-level conditions under which blocked-time cross-fitting plus orthogonality yields asymptotically normal inference for the target coefficient, and we provide a feasible variance estimator under unit clustering.

1.3 Roadmap

The remainder of the paper is organized as follows. Section 2 situates our contribution relative to the dynamic panel, semiparametric, and DML literatures, with a comparison table highlighting key methodological differences. Section 3 introduces the partially linear dynamic panel model and identifies the target parameter under transparent assumptions. Section 4 presents the orthogonal score construction and the cross-fitting algorithm, with explicit attention to dependence-aware fold design for panel data. Section 5 provides high-level asymptotic theory establishing asymptotic normality and feasible inference under weak dependence. Section 6 reports Monte Carlo evidence comparing the proposed estimator to naive plug-in approaches. Section 7 concludes and discusses extensions.

2 Related Literature

This paper sits at the intersection of (i) dynamic panel data econometrics, (ii) semiparametric/nonparametric estimation for partially linear models, and (iii) modern high-dimensional and machine-learning-assisted inference.

2.1 Dynamic panel data and inference with unobserved heterogeneity

Dynamic panels with unit fixed effects are a classical workhorse for modeling persistence and adjustment dynamics. A central complication is the interaction between fixed effects and lagged dependent variables, which generates finite-T bias under within transformations [Nickell, 1981]. A major line of research develops moment-based estimators that difference out fixed effects and use

lagged levels (and related transformations) as instruments, with specification testing and practical guidance [Arellano and Bond, 1991]. Extensions include alternative instrument constructions for error-components models and additional moment restrictions to improve finite-sample behavior [Arellano and Bover, 1995, Blundell and Bond, 1998]. These contributions define the baseline problem: inference on dynamic or policy parameters in panels must account for dependence and nuisance structure even before introducing modern high-dimensional controls.

2.2 Partially linear and semiparametric foundations

The model studied here is a partially linear dynamic panel in which the target parameter enters linearly while nuisance components may be unknown and nonlinear. Semiparametric partially linear regression and its orthogonalization logic have deep roots. In the i.i.d. setting, partialling-out ideas yield root-n consistent estimation of the linear component while allowing flexible nuisance estimation [Robinson, 1988]. This orthogonalization perspective is central to modern debiased/orthogonal-score approaches: the target estimator should be locally insensitive to nuisance perturbations, so that nuisance estimation error enters only at second order.

2.3 High-dimensional controls, regularization bias, and post-selection inference

A separate literature studies estimation and inference when the dimension of covariates is large relative to sample size, necessitating regularization (e.g., ℓ_1-penalization). Regularization is effective for prediction but can induce bias that can distort naive Wald inference on low-dimensional parameters of interest. In the context of treatment effect and structural inference with high-dimensional controls, one influential approach uses orthogonal moment equations and careful selection/regularization to obtain valid inference on low-dimensional targets [Belloni et al., 2014]. This motivates the basic methodological requirement for our problem: we must decouple inference on the parameter of interest from bias introduced by high-dimensional nuisance learning.

2.4 Double/debiased machine learning and cross-fitting

Double/debiased machine learning (DML) provides a general recipe for valid inference on low-dimensional parameters in the presence of high-dimensional or nonparametric nuisance functions. The key ingredients are Neyman-orthogonal score construction and sample splitting with cross-fitting, which jointly mitigate regularization bias and overfitting effects [Chernozhukov et al., 2018]. The DML framework has been widely adopted in empirical work because it is modular with respect to the choice of ML learner while delivering asymptotically normal estimators under appropriate rates.

Our paper adapts these ideas to a dynamic panel setting, where dependence and dynamics raise two practical issues. First, folds for cross-fitting must be chosen to respect serial dependence and the dynamic structure of the nuisance regressions. Second, the nuisance learning problems often resemble forecasting tasks (e.g., conditional mean estimation given lags), where time-series

cross-validation and lag selection require special care in practice. For time series, validation should respect time ordering; naive i.i.d. cross-validation can be misleading.

Table 1 summarizes how our approach differs from existing methods by comparing key methodological features across five strands of literature. The main differentiator is that we provide a complete framework that simultaneously handles (i) dynamic panel structure with fixed effects, (ii) high-dimensional or ML-based nuisance estimation, (iii) serial dependence through blocked-time cross-fitting, and (iv) feasible cluster-robust inference.

Table 1: Comparison of methodological approaches to inference with high-dimensional controls

	Setting	**Dependence handled?**	**Dynamic FE?**	**Cross-fitting scheme?**	**Orthogonal score?**	**Feasible variance?**
DML for i.i.d. settings (Chernozhukov et al., 2018)	i.i.d.	No	No	i.i.d. random folds	Yes	Yes
DML for dependent time series (emerging literature)	Time series	Yes (weak)	No	Time-blocked folds	Yes	Yes
High-dimensional/debiased for panels (Belloni et al., 2014)	Cross-section or i.i.d.	No	No	Not required (or i.i.d. folds)	Yes	Yes
Dynamic panel inference (classic: Arellano-Bond, etc.)	Panel	Yes (weak)	Yes	Not applicable (no ML nuisance)	No	Yes
This paper	**Panel**	**Yes (weak)**	**Yes**	**Blocked-time folds**	**Yes**	**Yes (cluster-robust)**

The table highlights that existing DML methods either assume i.i.d. observations (which fails in dynamic panels) or focus on time series without fixed effects (which omits the panel structure). Classical dynamic panel methods, while handling dependence and fixed effects, are not designed for ML-based nuisance estimation and do not employ orthogonal scores or cross-fitting. Our contribution is to combine these elements: we adapt the orthogonal score framework to dynamic panels, design cross-fitting that respects both serial dependence and unit clustering, and provide feasible variance estimation that accounts for the resulting dependence structure. This combination enables valid inference on dynamic causal parameters when nuisance functions are estimated with modern machine learning methods.

2.5 Positioning and incremental contribution

Relative to the dynamic panel literature, our focus is not on proposing yet another low-dimensional estimator of ρ_0 or θ_0 under parametric nuisance structure. Instead, we study inference for a dynamic causal parameter in the presence of rich, potentially nonlinear confounding captured by high-dimensional controls. Relative to the DML literature, our emphasis is on an implementable orthogonal-score construction and cross-fitting scheme tailored to dynamic panels and time dependence. The goal is to provide a template that practitioners can use when they need (i) dynamic structure, (ii) fixed effects, and (iii) high-dimensional or ML-based nuisance adjustment, while preserving valid inference for the policy parameter of interest.

3 Model and Assumptions

3.1 Panel setup and notation

Timing and conditioning. All conditions and conditional expectations are understood with respect to information available at (i,t), including histories of the outcome, treatment, and controls. We treat D_{it} as contemporaneously determined in the baseline exposition and impose an explicit conditional orthogonality restriction on the within disturbance—a conditional mean independence condition of the form $\mathbb{E}[\ddot{U}_{it} \mid \ddot{D}_{it}, W_{it}] = 0$—under which θ_0 is identified by the residualized moment in (4) (Assumption 3).

We observe a panel $\{(Y_{it}, D_{it}, X_{it}) : i = 1, \dots, N;\ t = 1, \dots, T\}$, where $Y_{it} \in \mathbb{R}$ is the outcome, $D_{it} \in \mathbb{R}$ is a scalar treatment/policy regressor, and $X_{it} \in \mathbb{R}^p$ is a potentially high-dimensional vector of controls (with p possibly larger than NT). For each unit i, define the unit-specific time average $\bar{A}_i = T^{-1} \sum_{t=1}^{T} A_{it}$ and the within-transformed variable

$$\ddot{A}_{it} := A_{it} - \bar{A}_i.$$

We apply this demeaning for all $t = 1, \dots, T$. The dynamic model in levels uses $t = 2, \dots, T$ because it contains $Y_{i,t-1}$, while the DML estimator uses only times for which the full lag window entering W_{it} exists: letting $L_* := \max\{L_y, L_d, L_x\}$, the usable time index set is $\mathcal{T}_{\text{use}} := \{L_* + 1, \dots, T\}$. Using a restricted mean over $t \in \mathcal{T}_{\text{use}}$ (with normalization $(T - L_*)^{-1}$) instead would only change the within transformation by $O(1/T)$ and does not affect the large-T asymptotic arguments. We use within transformation primarily to remove unit fixed effects, while allowing flexible nuisance adjustment via machine learning.

Throughout, we focus on inference for a low-dimensional structural parameter (the treatment effect), while treating high-dimensional functions of X_{it} and other conditional expectations as nuisance objects. To keep exposition tight, the main theory is stated for a balanced panel and $T \geq 3$. In applications the panel can be unbalanced due to missingness; our implementation computes within means using the available periods for each unit and reports the resulting usable n after lag construction and missingness. Section 7 discusses extensions and caveats for unbalancedness.

3.2 Partially linear dynamic panel model

The structural model is a partially linear dynamic panel with unit effects:

$$Y_{it} = \rho_0 Y_{i,t-1} + \theta_0 D_{it} + g_0(X_{it}) + \alpha_i + U_{it}, \qquad i = 1, \dots, N,\ t = 2, \dots, T, \tag{2}$$

where α_i is an unobserved time-invariant effect, U_{it} is an idiosyncratic disturbance, and $g_0(\cdot)$ is an unknown (possibly nonlinear) function. The parameter of interest is θ_0, which can be interpreted as a structural parameter (or, under additional sequential ignorability conditions, a causal effect) as discussed below.

Target parameter choice (what we estimate). In the main text we target θ_0 only and treat the dynamic component $\rho_0 Y_{i,t-1}$ as part of the high-dimensional information set W_{it} rather than an estimand. This keeps the partially linear score focused on the treatment effect and avoids bundling finite-T bias corrections for ρ_0 into the construction of the score for θ_0. Lagged outcomes enter W_{it} and are flexibly controlled for by the nuisance learners; joint estimation of (ρ_0, θ_0) is feasible as an extension (Section 4), but it is not the focus of the main results.

Applying within transformation to (2) yields

$$\ddot{Y}_{it} = \rho_0 \ddot{Y}_{i,t-1} + \theta_0 \ddot{D}_{it} + \ddot{g}_0(X_{it}) + \ddot{U}_{it}, \qquad t = 2, \ldots, T, \tag{3}$$

where $\ddot{g}_0(X_{it}) := g_0(X_{it}) - T^{-1} \sum_{s=1}^{T} g_0(X_{is})$ and analogously for $\ddot{U}_{it}$. Equation (3) removes the fixed effect but introduces the usual dynamic panel complication: $\ddot{Y}_{i,t-1}$ can be correlated with $\ddot{U}_{it}$ in finite samples, producing the classic Nickell bias when T is small [Nickell, 1981]. Moreover, this within-induced endogeneity is not confined to inference on ρ_0: if $\ddot{Y}_{i,t-1}$ is included in W_{it}, it can violate the conditional mean restriction used to identify θ_0 unless the resulting contamination is asymptotically negligible for the θ_0 moment. Our theoretical development is therefore framed under large-N, large-T asymptotics in which Nickell-type correlations vanish fast enough that their impact on $\hat{\theta}$ is $o(N^{-1/2})$ (see Assumption 4 and Corollary 1 below). Section 7 discusses how the orthogonal-score approach here can be combined with moment-based dynamic panel methods for short panels.

3.3 Identification target via orthogonal moments

The DML construction proceeds by rewriting the within-transformed model as a partially linear regression in which the treatment effect is identified by an orthogonal (Neyman-orthogonal) moment. For intuition, define a generic information set W_{it} that collects the observables used for nuisance adjustment. A convenient choice is

$$W_{it} := \big(\ddot{Y}_{i,t-1:t-L_y},\ \ddot{D}_{i,t-1:t-L_d},\ \ddot{X}_{i,t:t-L_x}\big),$$

where $L_y, L_d, L_x \geq 1$ are lag depths (with baseline $L_y = L_d = L_x = 1$) and $\ddot{X}_{i,t:t-L_x}$ includes contemporaneous X_{it} and its lags. Richer lag structures or transformations can be included. Including treatment and covariate histories is important in dynamic settings: persistence in D_{it} and time-varying confounding can make lagged determinants of D_{it} and Y_{it} predictive of current outcomes, so omitting histories from W_{it} risks omitted-history bias in the nuisance regressions. Let

$$\ell_0(W_{it}) := \mathbb{E}[\ddot{Y}_{it} \mid W_{it}], \qquad m_0(W_{it}) := \mathbb{E}[\ddot{D}_{it} \mid W_{it}],$$

and define residualized variables

$$\tilde{Y}_{it} := \ddot{Y}_{it} - \ell_0(W_{it}), \qquad \tilde{D}_{it} := \ddot{D}_{it} - m_0(W_{it}).$$

Under Assumption 3, the target parameter θ_0 is characterized by the orthogonality condition

$$\mathbb{E}\big[\tilde{D}_{it}\,(\tilde{Y}_{it} - \theta_0 \tilde{D}_{it})\big] = 0. \tag{4}$$

Lemma 1 shows that this moment follows from the identification restriction in Assumption 3 and, together with overlap (Assumption 5), uniquely pins down θ_0. When W_{it} contains within-demeaned lagged outcomes such as $\ddot{Y}_{i,t-1}$, the conditional mean restriction in Assumption 3 can fail at fixed T due to Nickell-type correlation; Assumption 4 allows an $O(1/T)$ remainder, which implies (4) holds only approximately but is still sufficient for $\sqrt{N}$ inference when $\sqrt{N}/T \to 0$ (Corollary 1). The corresponding partialling-out score is $\psi\big((Y_{it}, D_{it}, X_{it}), \theta, \eta\big) = \tilde{D}_{it}(m)\big(\tilde{Y}_{it}(\ell) - \theta\,\tilde{D}_{it}(m)\big)$ with $\eta = (\ell, m)$ and $\tilde{Y}_{it}(\ell) := \ddot{Y}_{it} - \ell(W_{it})$, $\tilde{D}_{it}(m) := \ddot{D}_{it} - m(W_{it})$. At (θ_0, η_0) it is Neyman-orthogonal: small perturbations of (ℓ, m) have no first-order effect on the moment, so nuisance estimation error enters only at second order [Chernozhukov et al., 2018].

Interpretation of θ_0. Assumption 3 imposes conditional mean independence of the within disturbance given $(\ddot{D}_{it}, W_{it})$, which, together with overlap (Assumption 5), identifies θ_0 via Lemma 1. In the absence of additional causal restrictions, θ_0 should be interpreted as a structural parameter characterizing the linear relationship between $\ddot{D}_{it}$ and $\ddot{Y}_{it}$ after controlling for W_{it} via the nuisance functions. When D_{it} is chosen in response to within-period shocks to Y_{it} that are not captured by W_{it}, the conditional mean independence restriction fails; in such cases, the framework should be combined with external instruments or policy discontinuities, replacing the partialling-out score with an orthogonal IV score.

Interpretation of θ_0: causal vs. structural. The notation and estimators are the same, but the language changes with assumptions:

- **Causal interpretation (when we use causal language).** We assume a level-*strict* exogeneity / ignorability primitive that is strong enough to survive the within transformation: conditional on the unit effect α_i and a sufficiently rich history H_{it} (chosen so that W_{it} is a function of H_{it}), the entire treatment path is mean-independent of the contemporaneous disturbance, so that the reduced-form restriction in Assumption 3 holds after demeaning. In dynamic panels where W_{it} contains within-demeaned lagged outcomes, within demeaning can still induce Nickell-type violations at fixed T; we therefore rely on the approximate orthogonality regime in Assumption 4 (and $\sqrt{N}/T \to 0$) when giving θ_0 a causal interpretation.

- **Structural interpretation (baseline).** Without sequential ignorability, θ_0 is a structural association: a partialling-out coefficient in the dynamic panel model after controlling flexibly for W_{it} and fixed effects.

- **What this framework does not solve.** Endogenous policy/treatment choice, simultaneity between D_{it} and Y_{it} within period, measurement error in D_{it} or Y_{it}, and macro common shocks that jointly move D_{it} and Y_{it}. Addressing these requires additional design features (e.g., instruments, discontinuities, or external shocks).

3.4 Assumptions

We state assumptions in a form that supports high-level theory and guides implementation.

Definition 1 (Effective sample size)**.** Let $L_* := \max\{L_y, L_d, L_x\}$ denote the maximum lag depth used in the feature vector W_{it} (treated as fixed for asymptotics). Let $n := N(T - L_*)$ denote the number of usable observations for $t \in \mathcal{T}_{\text{use}} = \{L_* + 1, \ldots, T\}$. In unbalanced panels (due to missingness), a natural analog is $n := \sum_{i=1}^{N} |\mathcal{T}_{i,\text{use}}|$, the total number of unit–time observations remaining after lag construction and missingness; our empirical tables report this n.

Assumption 1 (Asymptotic regime)**.** We consider a large-N asymptotic framework where $N \to \infty$ and $T \to \infty$ (large-N, large-T panel regime). The number of folds K is fixed. Let L_* be as in Definition 1 (treated as fixed for asymptotics). For the blocked-time fold construction with buffer, we introduce an additional separation buffer length $B_T \geq 0$ (an integer that may depend on T) satisfying:

- $B_T \to \infty$ as $T \to \infty$, and
- $B_T/T \to 0$ as $T \to \infty$.

Define the *effective* buffer used to construct training and buffer sets as

$$B_{T,*} := B_T + L_*,$$

so $B_{T,*} \to \infty$ and $B_{T,*}/T \to 0$ also hold when L_* is fixed. This ensures the effective buffer grows slowly relative to T, so training and test blocks remain of order T. For the blocked-time fold construction to be well-defined, we require T to be sufficiently large relative to K and $B_{T,*}$ (e.g., $T \geq 2K + 2B_{T,*}$ ensures each fold contains at least 2 time periods after accounting for buffers). The case $B_T = 0$ corresponds to "no additional dependence buffer" beyond the lag purge (i.e., $B_{T,*} = L_*$). Accommodating $B_T = 0$ requires additional boundary arguments for the dependence control, so our main theory is stated for $B_T \to \infty$. Algorithm 1 therefore defaults to a growing buffer rule such as $B = \lceil \log T \rceil$, while allowing $B = 0$ only as a short-T stress-test/heuristic setting that we study in simulations.

Additional growth for within-demeaned lagged outcomes. When the information set W_{it} includes within-demeaned lagged outcomes (e.g., $\ddot{Y}_{i,t-1}$), we additionally require $\sqrt{N}/T \to 0$ to make Nickell-type contamination asymptotically negligible for $\sqrt{N}$ inference on θ_0; see Assumption 4.

Practical alignment with the asymptotic regime. Theorems in Section 5 rely on $B_T \to \infty$ and weak serial dependence to make leakage across folds asymptotically negligible. In very short panels (e.g., $T = 8$) nontrivial buffering can be infeasible, so short-T results should be viewed as stress tests illustrating the tradeoff between fold purity and nuisance-learning precision rather than as evidence in favor of using no buffer in general.

Assumption 2 (Cross-sectional sampling and weak time dependence)**.** Across units $i = 1, \ldots, N$, the panel processes

$$\left\{(Y_{it}, D_{it}, X_{it}, \alpha_i, U_{it})_{t=1}^{T}\right\}_{i=1}^{N}$$

are independent and identically distributed. Within each unit i, the process $(Y_{it}, D_{it}, X_{it}, U_{it})$ is strictly stationary in t and exhibits weak serial dependence. Specifically, we assume α-mixing (or β-mixing) with mixing coefficients $\alpha(j)$ (or $\beta(j)$) that satisfy $\sum_{j=1}^{\infty} j\,\alpha(j)^{1-2/q} < \infty$ (or analogous condition for β-mixing) for some $q > 4$. Moreover, $\mathbb{E}[|U_{it}|^q] < \infty$ and $\mathbb{E}[\|X_{it}\|^q] < \infty$ for some $q > 4$. Under the buffer construction with B_T as in Assumption 1, we require that $\alpha(B_T) \to 0$ as $T \to \infty$, ensuring that dependence between observations separated by at least B_T periods becomes negligible. *Lag purge:* since the effective buffer is $B_{T,*} = B_T + L_*$ with fixed L_*, the same condition implies $\alpha(B_{T,*}) \to 0$.

Assumption 3 (Partially linear model and exogeneity)**.** After within-demeaning, we maintain the following reduced-form partially linear representation for the within-transformed process (motivated by (3) but not requiring an exact algebraic decomposition):

$$\ddot{Y}_{it} = \theta_0 \ddot{D}_{it} + h_0(W_{it}) + \ddot{U}_{it},$$

where $W_{it} := \left(\ddot{Y}_{i,t-1:t-L_y},\ \ddot{D}_{i,t-1:t-L_d},\ \ddot{X}_{i,t:t-L_x}\right)$ as defined in Algorithm 1 and $h_0(\cdot)$ is unknown. We impose the identification restriction (conditional mean independence / selection on observables for the within disturbance):

$$\mathbb{E}[\ddot{U}_{it} \mid \ddot{D}_{it}, W_{it}] = 0 \quad \text{a.s.}$$

Define

$$\ell_0(W_{it}) := \mathbb{E}[\ddot{Y}_{it} \mid W_{it}], \qquad m_0(W_{it}) := \mathbb{E}[\ddot{D}_{it} \mid W_{it}],$$

and the residualized variables

$$\tilde{Y}_{it} := \ddot{Y}_{it} - \ell_0(W_{it}), \qquad \tilde{D}_{it} := \ddot{D}_{it} - m_0(W_{it}).$$

This restriction implies $\mathbb{E}[\ddot{U}_{it}\tilde{D}_{it} \mid W_{it}] = 0$ a.s., and $\mathbb{E}[\ddot{U}_{it} \mid W_{it}] = 0$ follows by iterated expectations. Define the treatment equation

$$\ddot{D}_{it} = m_0(W_{it}) + \ddot{V}_{it},$$

with $\ddot{V}_{it} := \tilde{D}_{it}$, so $\mathbb{E}[\ddot{V}_{it} \mid W_{it}] = 0$ holds by definition. Under the restriction above, $\ell_0(W_{it}) =$

$\theta_0 m_0(W_{it}) + h_0(W_{it})$, and Lemma 1 shows that (4) holds and, with Assumption 5, identifies θ_0.

Assumption 4 (Nickell-type approximate orthogonality when W_{it} includes $\ddot{Y}_{i,t-1}$)**.** In dynamic panels, within demeaning typically induces $\mathrm{Corr}(\ddot{Y}_{i,t-1}, \ddot{U}_{it}) \neq 0$ in finite samples [Nickell, 1981, Hahn and Kuersteiner, 2002]. To allow for this while maintaining $\sqrt{N}$ inference on θ_0, suppose that when W_{it} includes within-demeaned lagged outcomes,

$$\mathbb{E}[\ddot{U}_{it} \mid \ddot{D}_{it}, W_{it}] = r_{it,T}$$

for some (possibly unknown) remainder $r_{it,T}$ satisfying $\|r_{it,T}\|_2 \leq C/T$ uniformly in t for a constant $C < \infty$, and that $\sqrt{N}/T \to 0$ as $N, T \to \infty$.

Lemma 1 (Identification via partialling-out orthogonality)**.** *Under Assumption 3, the orthogonality condition (4) holds at θ_0. If Assumption 5 also holds, then θ_0 is the unique solution to (4) and satisfies $\theta_0 = \mathbb{E}[\tilde{D}_{it}\tilde{Y}_{it}]/\mathbb{E}[\tilde{D}_{it}^2]$.*

Proof. From the within model, $\ddot{Y}_{it} = \theta_0 \ddot{D}_{it} + h_0(W_{it}) + \ddot{U}_{it}$. By definition, $\ell_0(W_{it}) = \mathbb{E}[\ddot{Y}_{it} \mid W_{it}]$ and $m_0(W_{it}) = \mathbb{E}[\ddot{D}_{it} \mid W_{it}]$, and Assumption 3 implies $\mathbb{E}[\ddot{U}_{it} \mid W_{it}] = 0$. Hence $\ell_0(W_{it}) = \theta_0 m_0(W_{it}) + h_0(W_{it})$, so $\tilde{Y}_{it} - \theta_0 \tilde{D}_{it} = \ddot{U}_{it}$. Then

$$\mathbb{E}[\tilde{D}_{it}(\tilde{Y}_{it} - \theta_0 \tilde{D}_{it})] = \mathbb{E}[\tilde{D}_{it}\ddot{U}_{it}] = \mathbb{E}\Big[\mathbb{E}[\ddot{D}_{it}\ddot{U}_{it} \mid W_{it}] - m_0(W_{it})\mathbb{E}[\ddot{U}_{it} \mid W_{it}]\Big] = 0,$$

where $\mathbb{E}[\ddot{D}_{it}\ddot{U}_{it} \mid W_{it}] = \mathbb{E}[\ddot{D}_{it}\mathbb{E}[\ddot{U}_{it} \mid \ddot{D}_{it}, W_{it}] \mid W_{it}] = 0$ by Assumption 3. For uniqueness, $\mathbb{E}[\tilde{D}_{it}(\tilde{Y}_{it} - \theta\tilde{D}_{it})] = \mathbb{E}[\tilde{D}_{it}\tilde{Y}_{it}] - \theta\mathbb{E}[\tilde{D}_{it}^2]$ has slope $-\mathbb{E}[\tilde{D}_{it}^2]$, which is bounded away from zero by Assumption 5. □

Remark 1 (From causal primitives to Assumption 3). Assumption 3 is a reduced-form restriction on the within disturbance. Because within-demeaning replaces (U_{it}, D_{it}, W_{it}) by $(\ddot{U}_{it}, \ddot{D}_{it}, W_{it})$ and uses unit means computed over the full time path, the mapping from level assumptions to Assumption 3 is not automatic.

A sufficient (and standard) primitive is a *strict exogeneity* condition in levels that conditions on the whole treatment path, for example

$$\mathbb{E}[U_{it} \mid D_{i1:T}, H_{iT}, \alpha_i] = 0 \quad \text{for all } t,$$

with W_{it} measurable with respect to H_{iT}. This type of condition implies $\mathbb{E}[\ddot{U}_{it} \mid \ddot{D}_{it}, W_{it}] = 0$ after within transformation.

By contrast, a period-by-period sequential ignorability condition such as $\mathbb{E}[U_{it} \mid D_{it}, H_{it}, \alpha_i] = 0$ may fail to imply Assumption 3 even when $L_y = 0$, because $\ddot{D}_{it}$ and W_{it} inherit dependence on the full time path through unit means. If one wants to rely on such weaker primitives, an additional large-T approximation argument is needed to control the demeaning-induced dependence for all within-transformed regressors; the paper formalizes this type of $O(1/T)$ remainder only for within-demeaned lagged outcomes via Assumption 4.

Assumption 5 (Overlap / relevance)**.** There exists $c > 0$ such that

$$\mathbb{E}\Big[\tilde{D}_{it}^2\Big] \geq c \quad \text{and} \quad \mathbb{E}\Big[\tilde{D}_{it}^2 \mid W_{it}\Big] \geq c \text{ a.s.}$$

Assumption 6 (Nuisance regularity and learnability)**.** The nuisance functions ℓ_0 and m_0 belong to a function class that can be learned by ML methods in mean-square error. Let $\hat{\ell}^{(-k)}$ and $\hat{m}^{(-k)}$ be the cross-fitted ML estimators for fold k defined in Algorithm 1 (Section 4). They satisfy, for some deterministic sequences $\delta_{Y,n}, \delta_{D,n} \to 0$,

$$\|\hat{\ell}^{(-k)} - \ell_0\|_2 = O_p(\delta_{Y,n}), \qquad \|\hat{m}^{(-k)} - m_0\|_2 = O_p(\delta_{D,n}),$$

uniformly over folds $k = 1, \ldots, K$, where the L_2 norm is taken over the distribution of W_{it}. The product-rate condition is

$$\delta_{Y,n}\, \delta_{D,n} = o(n^{-1/2}).$$

These rates are understood to hold under the dependent-data setting (Assumption 2), accounting for the fact that training samples within folds exhibit serial dependence.

Remark 2 (Learnability under dependence is a high-level assumption). Assumption 6 is stated at a high level: it isolates the estimator's requirements from the conditions under which a particular learner achieves those rates. For sparse linear learners (e.g., Lasso) under weak dependence, rate results are available under mixing or related dependence conditions; see, for example, Wu and Wu [2016] and Basu and Michailidis [2015]. For nonlinear learners (e.g., trees/boosting), sharp L_2 rates under dependent sampling are less settled, so in those cases Assumption 6 should be read as an explicit learnability requirement rather than an automatic guarantee.

Remark 3 (Why product rates). The product-rate condition is standard in orthogonal-score estimation: it permits each nuisance to converge relatively slowly (as with regularized ML), while still making their combined impact on the target estimator asymptotically negligible because it enters at second order.

Remarks on Nickell bias and within-demeaning with lagged outcomes. The estimator uses within-demeaning to remove fixed effects, and the information set W_{it} includes the within-demeaned lagged outcome $\ddot{Y}_{i,t-1}$. In finite samples with small T, the correlation between $\ddot{Y}_{i,t-1}$ and $\ddot{U}_{it}$ can produce Nickell bias [Nickell, 1981]. Thus, even under sequential ignorability conditions stated in levels, Assumption 3 is not automatic once W_{it} contains $\ddot{Y}_{i,t-1}$: conditioning on W_{it} can inherit the within-induced endogeneity. Assumption 4 formalizes the regime we rely on when $\ddot{Y}_{i,t-1}$ is included in W_{it}: the induced violation of conditional mean independence enters the orthogonal score as a bias of order $1/T$, so $\sqrt{N}$-valid inference requires $\sqrt{N}/T \to 0$ (Corollary 1). In very short panels (T small and fixed), the method should be combined with moment-based dynamic panel techniques; see Section 7 for discussion.

3.5 Discussion

Assumptions 1, 2, 3, 5, and 6 formalize the environment we have in mind: a large panel with weak serial dependence and potentially very rich controls, where the treatment effect is identified by an orthogonal moment after residualizing both outcome and treatment on a (possibly high-dimensional) information set. The remaining task is to provide an explicit orthogonal score, a dependence-aware cross-fitting scheme, and feasible variance estimation. These are developed in Sections 4 and 5.

4 Estimation Algorithm

This section presents an implementable estimator for θ_0 based on an orthogonal score and cross-fitting. The construction follows the general DML recipe [Chernozhukov et al., 2018], but we emphasize fold designs that are appropriate for dynamic panels.

For convenience, the full estimator and inference pipeline is summarized in the following recipe.

Estimator recipe (blocked-time cross-fitted DML with buffer).
Inputs: panel $\{(Y_{it}, D_{it}, X_{it}) : i = 1, \dots, N;\ t = 1, \dots, T\}$; number of folds K; additional buffer length $B \geq 0$ (default $B = \lceil \log T \rceil$); ML learner; lag depths $L_y, L_d, L_x \geq 1$.
Estimand: θ_0 characterized by $\mathbb{E}[\psi(\cdot, \theta_0, \eta_0)] = 0$, where $\eta_0 = (\ell_0, m_0)$ (identification follows from Assumption 3 and Lemma 1).
Nuisances: $\ell_0(w) := \mathbb{E}[\ddot{Y}_{it} \mid W_{it} = w]$ and $m_0(w) := \mathbb{E}[\ddot{D}_{it} \mid W_{it} = w]$.
Orthogonal score: with $\eta = (\ell, m)$, $\tilde{Y}_{it}(\ell) := \ddot{Y}_{it} - \ell(W_{it})$, $\tilde{D}_{it}(m) := \ddot{D}_{it} - m(W_{it})$, and

$$\psi\big((Y_{it}, D_{it}, X_{it}), \theta, \eta\big) := \tilde{D}_{it}(m)\,\big(\tilde{Y}_{it}(\ell) - \theta\,\tilde{D}_{it}(m)\big).$$

1. **Step 0 (within/FE step and features).** Within-demean to obtain $\ddot{Y}_{it}$ and $\ddot{D}_{it}$ and construct $W_{it} = \big(\ddot{Y}_{i,t-1:t-L_y},\ \ddot{D}_{i,t-1:t-L_d},\ \ddot{X}_{i,t:t-L_x}\big)$. Let $L_* := \max\{L_y, L_d, L_x\}$ and let the usable time index set be $\mathcal{T}_{\text{use}} := \{L_* + 1, \dots, T\}$. Let $\mathcal{I} = \{(i,t) : i = 1, \dots, N;\ t \in \mathcal{T}_{\text{use}}\}$.

2. **Step 1 (blocked-time folds with buffer).** Partition $\mathcal{T}_{\text{use}}$ into K contiguous blocks $\{\mathcal{T}_k\}_{k=1}^K$. For each fold k, define buffer times with an effective buffer $B_* := B + L_*$, $\mathcal{G}_k(B_*) := \{t \in \mathcal{T}_{\text{use}} : \min_{s \in \mathcal{T}_k} |t - s| \leq B_*\} \setminus \mathcal{T}_k$, training times $\mathcal{J}_k(B_*) := \mathcal{T}_{\text{use}} \setminus (\mathcal{T}_k \cup \mathcal{G}_k(B_*))$, fold test set $\mathcal{I}_k := \{(i,t) \in \mathcal{I} : t \in \mathcal{T}_k\}$, and fold training set $\mathcal{J}_k := \{(i,t) : i = 1, \dots, N;\ t \in \mathcal{J}_k(B_*)\}$.

3. **Step 2 (fit nuisances).** For each k, fit on $\mathcal{J}_k$: $\hat{\ell}^{(-k)}(w)$ for $\mathbb{E}[\ddot{Y}_{it} \mid W_{it} = w]$ and $\hat{m}^{(-k)}(w)$ for $\mathbb{E}[\ddot{D}_{it} \mid W_{it} = w]$.

4. **Step 3 (residualize and score).** For each $(i,t) \in \mathcal{I}_k$ set $\hat{\tilde{Y}}_{it} := \ddot{Y}_{it} - \hat{\ell}^{(-k)}(W_{it})$ and

$\hat{\ddot{D}}_{it} := \ddot{D}_{it} - \hat{m}^{(-k)}(W_{it})$, and compute the score $\hat{\psi}_{it}(\theta) := \hat{\ddot{D}}_{it}\hat{\ddot{Y}}_{it} - \theta\,\hat{\ddot{D}}_{it}^2$ (equivalently, $\hat{\psi}_{it}(\theta) = \hat{\ddot{D}}_{it}(\hat{\ddot{Y}}_{it} - \theta\,\hat{\ddot{D}}_{it})$).

5. **Step 4 (solve pooled moment).** Compute the pooled estimator

$$\hat{\theta} := \frac{\sum_{(i,t)\in\mathcal{I}} \hat{\ddot{D}}_{it}\hat{\ddot{Y}}_{it}}{\sum_{(i,t)\in\mathcal{I}} \hat{\ddot{D}}_{it}^2},$$

equivalently $\hat{\theta}$ solves $\sum_{(i,t)\in\mathcal{I}} \hat{\psi}_{it}(\theta) = 0$. (Optionally, report fold-specific slopes $\hat{\theta}_k := \frac{\sum_{(i,t)\in\mathcal{I}_k} \hat{\ddot{D}}_{it}\hat{\ddot{Y}}_{it}}{\sum_{(i,t)\in\mathcal{I}_k} \hat{\ddot{D}}_{it}^2}$ as diagnostics.)

6. **Step 5 (unit-clustered variance and CI).** Let $n = N(T - L_*)$ and define $\hat{\psi}_{it} := \hat{\ddot{D}}_{it}\left(\hat{\ddot{Y}}_{it} - \hat{\theta}\,\hat{\ddot{D}}_{it}\right) = \hat{\ddot{D}}_{it}\hat{\ddot{Y}}_{it} - \hat{\theta}\,\hat{\ddot{D}}_{it}^2$, $\hat{J} := -\frac{1}{n}\sum_{(i,t)\in\mathcal{I}} \hat{\ddot{D}}_{it}^2$ and

$$\hat{V} := \hat{J}^{-2} \cdot \frac{1}{n^2} \sum_{i=1}^{N} \Big(\sum_{t\in\mathcal{T}_{\text{use}}} \hat{\psi}_{it} \Big)^2.$$

A $(1-\alpha)$ CI is $\hat{\theta} \pm z_{1-\alpha/2}\sqrt{\hat{V}}$.

Implementation note. Practical guidance for choosing B and optional residualized-treatment trimming are given below in *Choosing the buffer length* and *Implementation details and robustness checks*.

Within-demeaning and fold purity. The within transformation in Step 0 is a deterministic linear filter applied once using all time periods; it removes fixed effects but does not itself involve ML fitting. Because the unit mean $\bar{A}_i = T^{-1}\sum_{t=1}^{T} A_{it}$ uses the full time path, global demeaning technically couples observations across time blocks and can induce mechanical correlation between a training-period within residual and shocks in a held-out test block. In our large-T framework, this induced train–test dependence is negligible: each held-out realization enters the training-period within residual only through $\bar{A}_i$ with weight $1/T$, so the extra cross-block covariance is of order $O(1/T)$ (see Appendix A.1.2). We therefore retain global demeaning (standard in FE panels) while guarding against overfitting through dependence-aware sample splitting for the ML nuisances. If strict fold purity is desired in finite samples, an optional fold-specific demeaning variant is described in the implementation notes below.

4.1 Orthogonal score

Let W_{it} denote the information set used for nuisance adjustment. A baseline choice is

$$W_{it} = \big(\ddot{Y}_{i,t-1:t-L_y},\ \ddot{D}_{i,t-1:t-L_d},\ \ddot{X}_{i,t:t-L_x}\big),$$

with lag depths $L_y, L_d, L_x \geq 1$ (baseline $L_y = L_d = L_x = 1$) and $\ddot{X}_{i,t:t-L_x}$ including contemporaneous X_{it} and its lags. Define the nuisance functions

$$\ell_0(w) := \mathbb{E}[\ddot{Y}_{it} \mid W_{it} = w], \qquad m_0(w) := \mathbb{E}[\ddot{D}_{it} \mid W_{it} = w].$$

Given candidate estimates (ℓ, m), define residualized variables

$$\tilde{Y}_{it}(\ell) := \ddot{Y}_{it} - \ell(W_{it}), \qquad \tilde{D}_{it}(m) := \ddot{D}_{it} - m(W_{it}).$$

We use the (partialling-out) orthogonal score for θ:

$$\psi\big((Y_{it}, D_{it}, X_{it}), \theta, \eta\big) := \tilde{D}_{it}(m)\,\Big(\tilde{Y}_{it}(\ell) - \theta\,\tilde{D}_{it}(m)\Big), \tag{5}$$

where $\eta = (\ell, m)$. The identifying equation is $\mathbb{E}[\psi(\cdot, \theta_0, \eta_0)] = 0$ with $\eta_0 = (\ell_0, m_0)$, with identification guaranteed by Assumption 3 and Lemma 1.

A key property is Neyman orthogonality: small perturbations of the nuisance functions have no first-order effect on the moment condition at the truth. Formally, for suitable directions h,

$$\frac{\partial}{\partial r}\mathbb{E}\Big[\psi(\cdot, \theta_0, \eta_0 + rh)\Big]\Big|_{r=0} = 0.$$

This removes first-order sensitivity to regularization bias in ML nuisance estimates and is the basis for the product-rate condition in Assumption 6.

4.2 Cross-fitting under dependence

In i.i.d. settings, cross-fitting typically uses random folds. In panels with serial dependence, fold construction should avoid training on observations that are "too close" to test observations in time.

Let $L_* := \max\{L_y, L_d, L_x\}$ and let $\mathcal{T}_{\text{use}} := \{L_* + 1, \ldots, T\}$ be the usable time index set (so that all lagged histories entering W_{it} exist). Let $\mathcal{I} = \{(i,t) : i = 1, \ldots, N;\ t \in \mathcal{T}_{\text{use}}\}$ be the index set of usable observations. Partition $\mathcal{I}$ into K folds $\{\mathcal{I}_k\}_{k=1}^K$. We recommend one of the following dependence-aware fold schemes:

(A) Blocked-time folds with an optional buffer (default). Partition the usable time index $\mathcal{T}_{\text{use}}$ into K contiguous blocks $\{\mathcal{T}_k\}_{k=1}^K$ and set $\mathcal{I}_k := \{(i,t) \in \mathcal{I} : t \in \mathcal{T}_k\}$. This holds out entire time blocks, reducing leakage across folds when learning conditional expectations with lags. Algorithm 1 augments this scheme with an *additional* buffer parameter $B \geq 0$ to further reduce train–test dependence leakage. When evaluating fold k, define buffer times and training times using an *effective* buffer $B_* := B + L_*$, where $L_* := \max\{L_y, L_d, L_x\}$ is the maximum lag depth in W_{it}: with this choice, no training observation has a lagged feature window that overlaps the held-out test block. Setting $B = 0$ corresponds to "lag purge only" (effective buffer $B_* = L_*$) and should be read as a short-T stress-test/heuristic setting rather than as a theory-covered default. For

theoretical convenience under serial dependence, the asymptotic results in Section 5 are stated for buffer sequences B_T that grow slowly with T (so $\alpha(B_T) \to 0$). Algorithm 1 defaults to a growing rule such as $B = \lceil \log T \rceil$; we set $B = 0$ only in short-T stress-test simulations where additional buffering is infeasible. The informal description "leave-one-time-block-out with a buffer" refers to this same blocked-time fold scheme with $B > 0$.

4.2.1 Choosing the buffer length

Practical guidance for B is analogous to bandwidth or undersmoothing choices: larger buffers reduce train–test dependence leakage but shrink the effective training sample in each fold. Thus B trades off dependence control against nuisance-learning precision and may be infeasible when T is small and K is fixed. Our recommended default is the logarithmic rule $B = \lceil \log T \rceil$, which satisfies $B_T \to \infty$ and $B_T/T \to 0$ and is typically small in practice. Two simple theory-aligned rules that satisfy $B_T \to \infty$ and $B_T/T \to 0$ are

$$B_T = \lceil \log T \rceil \qquad \text{and} \qquad B_T = \lfloor \sqrt{T} \rfloor.$$

As a diagnostic alternative (heuristic, not part of the theory), choose B so that serial dependence is empirically small beyond lag B: compute the sample autocorrelation function of within-demeaned Y (or of residuals from a simple baseline regression) and select the smallest B such that $|\widehat{\rho}(\ell)| < 0.05$ for all $\ell \geq B$ over a reasonable lag range. This rule-of-thumb calibrates B to the observed persistence without altering the formal assumptions.

(B) Clustered-unit folds. If cross-sectional dependence is a concern (e.g., common shocks beyond α_i), one can instead hold out sets of units: partition $\{1, \ldots, N\}$ into $\{\mathcal{N}_k\}_{k=1}^K$ and set $\mathcal{I}_k := \{(i,t) \in \mathcal{I} : i \in \mathcal{N}_k\}$. This is conservative for strong common dependence.

In the remainder, we present the estimator for a generic fold partition.

4.3 Algorithm (DML partialling-out estimator)

Algorithm 1: Blocked-time cross-fitted DML for dynamic panels

Input: Panel $\{(Y_{it}, D_{it}, X_{it}) : i = 1, \ldots, N; t = 1, \ldots, T\}$, lag depths (L_y, L_d, L_x) (default $(1,1,1)$), number of folds K (default $K = 4$), additional buffer length $B \geq 0$ (default $B = \lceil \log T \rceil$; use $B = 0$ only as a short-T stress-test/heuristic), ML learner.

Step 1: Construct lagged histories and within-demean.

- For each unit i, compute lags $Y_{i,t-\ell}$ for $\ell = 1, \ldots, L_y$, $D_{i,t-\ell}$ for $\ell = 1, \ldots, L_d$, and $X_{i,t-\ell}$ for $\ell = 1, \ldots, L_x$.
- Within-demean Y_{it}, D_{it}, and the lagged histories by unit to obtain $\ddot{Y}_{it}$, $\ddot{D}_{it}$, $\ddot{Y}_{i,t-\ell}$, $\ddot{D}_{i,t-\ell}$, and $\ddot{X}_{i,t-\ell}$.

- Define
$$W_{it} := \big(\ddot{Y}_{i,t-1:t-L_y},\ \ddot{D}_{i,t-1:t-L_d},\ \ddot{X}_{i,t:t-L_x}\big),$$
and drop observations with $t \le \max\{L_y, L_d, L_x\}$.

Step 2: Construct blocked-time folds with buffer.

- Partition usable time periods $\{L_* + 1, \dots, T\}$ into K contiguous blocks $\{\mathcal{T}_k\}_{k=1}^K$ using equal-sized splits (or as close as possible).
- Define the maximum lag depth used in features: $L_* := \max\{L_y, L_d, L_x\}$, and the *effective buffer*
$$B_* := B + L_*.$$
Equivalently, B_* "purges" any training observation whose lagged feature window overlaps the held-out test block.
- For each fold k, define:
  - Test time indices: $\mathcal{T}_k$ (the k-th time block).
  - Buffer time indices: $\mathcal{G}_k(B_*) := \{t \in \{L_* + 1, \dots, T\} : \min_{s \in \mathcal{T}_k} |t - s| \le B_*\} \setminus \mathcal{T}_k$.
  - Training time indices: $\mathcal{J}_k(B_*) := \{L_* + 1, \dots, T\} \setminus (\mathcal{T}_k \cup \mathcal{G}_k(B_*))$.
- Define fold k test set as $\mathcal{I}_k := \{(i,t) : i = 1, \dots, N; t \in \mathcal{T}_k\}$.
- Define fold k training set as $\mathcal{J}_k := \{(i,t) : i = 1, \dots, N; t \in \mathcal{J}_k(B_*)\}$.
- *Note:* When $B = 0$, the remaining buffer is exactly the lag purge: $B_* = L_*$; this setting is used primarily as a short-T stress test.

Step 3: For each fold $k = 1, \dots, K$:

1. **Train nuisances on training set.** Using observations in $\mathcal{J}_k$ (the training set for fold k), fit ML regressions:
$$\hat{\ell}^{(-k)}(w) := \text{ML estimate of } \mathbb{E}[\ddot{Y}_{it} \mid W_{it} = w] \text{ on } \mathcal{J}_k,$$
$$\hat{m}^{(-k)}(w) := \text{ML estimate of } \mathbb{E}[\ddot{D}_{it} \mid W_{it} = w] \text{ on } \mathcal{J}_k.$$

2. **Compute residuals on held-out fold.** For each $(i,t) \in \mathcal{I}_k$:
$$\hat{\ddot{Y}}_{it} := \ddot{Y}_{it} - \hat{\ell}^{(-k)}(W_{it}), \qquad \hat{\ddot{D}}_{it} := \ddot{D}_{it} - \hat{m}^{(-k)}(W_{it}).$$

3. **Score on held-out fold.** For each $(i,t) \in \mathcal{I}_k$ define the score
$$\hat{\psi}_{it}(\theta) := \hat{\ddot{D}}_{it}\big(\hat{\ddot{Y}}_{it} - \theta\, \hat{\ddot{D}}_{it}\big) = \hat{\ddot{D}}_{it}\hat{\ddot{Y}}_{it} - \theta\, \hat{\ddot{D}}_{it}^2.$$

4. **Fold-specific estimate.**

$$\hat{\theta}_k := \frac{\sum_{(i,t)\in\mathcal{I}_k} \hat{\tilde{D}}_{it}\hat{\tilde{Y}}_{it}}{\sum_{(i,t)\in\mathcal{I}_k} \hat{\tilde{D}}_{it}^2}.$$

Step 4: Solve the pooled moment (equivalently, pool fold numerators/denominators):

$$\hat{\theta} := \frac{\sum_{k=1}^{K}\sum_{(i,t)\in\mathcal{I}_k} \hat{\tilde{D}}_{it}\hat{\tilde{Y}}_{it}}{\sum_{k=1}^{K}\sum_{(i,t)\in\mathcal{I}_k} \hat{\tilde{D}}_{it}^2}.$$

Output: $\hat{\theta}$ (point estimate). The final cross-fitted DML estimator is

$$\hat{\theta} := \frac{\sum_{(i,t)\in\mathcal{I}} \hat{\tilde{D}}_{it}\hat{\tilde{Y}}_{it}}{\sum_{(i,t)\in\mathcal{I}} \hat{\tilde{D}}_{it}^2}, \tag{6}$$

which solves the pooled score equation $\sum_{(i,t)\in\mathcal{I}} \hat{\psi}_{it}(\theta) = 0$. Fold-specific slopes $\{\hat{\theta}_k\}_{k=1}^{K}$ can be reported as diagnostics.

Implementation notes. The algorithm can be implemented with any supervised ML learner for the nuisance regressions, including Lasso (with cross-validation for regularization parameter selection), random forests, or other methods. The blocked-time fold construction separates training and test sets in time, reducing overfitting bias while remaining compatible with weak serial dependence under the mixing conditions. For variance estimation (described below), the score contributions $\hat{\psi}_{it}$ are evaluated at the final estimate $\hat{\theta}$ by recomputing residuals using the cross-fitted nuisance estimates, ensuring consistency of the variance estimator.

4.4 Variance estimation and inference

Let $\hat{\eta}$ denote the collection of cross-fitted nuisance estimates. Define the cross-fitted score contributions

$$\hat{\psi}_{it} := \psi\big((Y_{it}, D_{it}, X_{it}), \hat{\theta}, \hat{\eta}\big) = \hat{\tilde{D}}_{it}\Big(\hat{\tilde{Y}}_{it} - \hat{\theta}\,\hat{\tilde{D}}_{it}\Big).$$

Let

$$\hat{J} := -\frac{1}{n}\sum_{(i,t)\in\mathcal{I}} \hat{\tilde{D}}_{it}^2,$$

the sample Jacobian of the moment condition with respect to θ (with $n = N(T - L_*)$).

Cluster-robust variance by unit (default). The variance estimator accounts for within-unit serial dependence by clustering at the unit level. First, recompute score contributions at $\hat{\theta}$:

$$\hat{\psi}_{it} := \hat{\tilde{D}}_{it}\Big(\hat{\tilde{Y}}_{it} - \hat{\theta}\,\hat{\tilde{D}}_{it}\Big),$$

where $\hat{\ddot{Y}}_{it}$ and $\hat{\ddot{D}}_{it}$ are the cross-fitted residuals from the algorithm above. The Jacobian is

$$\hat{J} := -\frac{1}{n} \sum_{(i,t)\in\mathcal{I}} \hat{\ddot{D}}_{it}^2,$$

where $n = N(T - L_*)$ is the effective sample size. The unit-clustered variance estimator is

$$\hat{V} = \hat{J}^{-2} \cdot \frac{1}{n^2} \sum_{i=1}^{N} \left(\sum_{t\in\mathcal{T}_{\text{use}}} \hat{\psi}_{it} \right)^2.$$

This aggregates score contributions within each unit i before squaring, accounting for serial correlation within units while treating units as independent. A $(1-\alpha)$ confidence interval is

$$\hat{\theta} \pm z_{1-\alpha/2} \sqrt{\hat{V}}.$$

Block-robust alternatives. If dependence is primarily in time (common shocks), one can instead aggregate by time blocks and use a block-HAC style variance estimate. We leave a detailed exploration of optimal variance estimation under various dependence structures to future work; our simulations in Section 6 report the unit-clustered variance as a transparent baseline.

4.5 Implementation details

Within transformation and lag construction. We compute $\ddot{Y}_{it}$ and $\ddot{D}_{it}$ by demeaning within unit using $t = 1, \ldots, T$ (as in Section 3). Lags $\ddot{Y}_{i,t-1}$ are constructed prior to fold splitting.

Optional: fold-specific within demeaning for strict fold purity. To fully insulate each fold from the held-out block, one can replace global demeaning with a fold-specific transformation. For fold k, compute unit means using only the fold's training times $\mathcal{J}_k(B_*)$: for any variable A_{it} used in the estimator (including lagged histories that form W_{it}), set $\bar{A}_i^{(-k)} := |\mathcal{J}_k(B_*)|^{-1} \sum_{t\in\mathcal{J}_k(B_*)} A_{it}$ and define $\ddot{A}_{it}^{(-k)} := A_{it} - \bar{A}_i^{(-k)}$ for all $t \in \mathcal{J}_k(B_*) \cup \mathcal{T}_k$. Then train nuisances on $\{\ddot{A}_{it}^{(-k)} : t \in \mathcal{J}_k(B_*)\}$ and score on $\{\ddot{A}_{it}^{(-k)} : t \in \mathcal{T}_k\}$. This eliminates any use of held-out outcomes/treatments in the within transformation while leaving fixed effects removed (since α_i drops out under any time average).

Joint estimation of (ρ_0, θ_0). The above presentation targets θ_0 after absorbing the dynamic regressor into W_{it}. An alternative is to estimate (ρ_0, θ_0) jointly with a two-dimensional orthogonal score. For clarity, the main text focuses on inference for θ_0; Appendix A sketches the joint-score extension. Because the joint score includes $\ddot{Y}_{i,t-1}$ as a regressor, it inherits the usual Nickell-order endogeneity from within demeaning and therefore requires a large-T regime (e.g., $\sqrt{N}/T \to 0$) for $\sqrt{N}$ inference on (ρ_0, θ_0); see Appendix A.3.

Small-T considerations. When T is very small, Nickell-type bias may not be negligible for ρ_0. Moreover, if W_{it} includes within-demeaned lagged outcomes (e.g., $\ddot{Y}_{i,t-1}$), the same within-induced

endogeneity can contaminate the orthogonality condition used for θ_0 unless T is large enough that the resulting bias is $o(N^{-1/2})$ (Assumption 4). For genuinely short panels, combining this DML partialling-out approach with classical moment restrictions for dynamics (e.g., difference or system GMM) is a promising direction.

Recommended default pipeline. A practical default is: (i) within-demean (Y_{it}, D_{it}, X_{it}) by unit; (ii) choose W_{it} to include key outcome, treatment, and covariate histories (at least $\ddot{Y}_{i,t-1}$ and $\ddot{D}_{i,t-1}$) and transformations of X_{it}; (iii) construct blocked-time folds with a growing additional buffer such as $B = \lceil \log T \rceil$ (set $B = 0$ only as a short-T stress-test/heuristic); (iv) fit nuisance regressions for $\mathbb{E}[\ddot{Y}_{it} \mid W_{it}]$ and $\mathbb{E}[\ddot{D}_{it} \mid W_{it}]$ using a regularized linear learner (Lasso) as a baseline and optionally a nonlinear learner (random forests/boosting) as a robustness check; (v) compute cross-fitted residuals and form $\hat{\theta}$; and (vi) report unit-clustered inference by default, plus time-clustered or two-way clustered inference if aggregate shocks are salient.

Implementation details and robustness checks. A practical robustness safeguard in the partialling-out score is to inspect the residualized treatment $\hat{\ddot{D}}_{it}$ for weak variation and extreme values that can dominate the score $\hat{\psi}_{it} = \hat{\ddot{D}}_{it}(\hat{\ddot{Y}}_{it} - \hat{\theta}\hat{\ddot{D}}_{it})$. First, flag low-variation blocks: for each held-out time block $\mathcal{T}_k$, compute $\widehat{\mathrm{Var}}(\hat{\ddot{D}}_{it} : t \in \mathcal{T}_k)$ and flag if below ε (e.g., $\varepsilon = 10^{-6}\widehat{\mathrm{Var}}(\hat{\ddot{D}})$; if $\hat{\ddot{D}}$ is roughly standardized, $\varepsilon = 10^{-8}$ is a conservative fixed choice). Second, compute standardized residualized treatment

$$z_{it} := \frac{\hat{\ddot{D}}_{it}}{\widehat{\mathrm{sd}}(\hat{\ddot{D}})},$$

and trim observations with $|z_{it}| > c$ using either a high-quantile rule (default $c = Q_{0.995}(|z|)$, with $Q_{0.999}$ as a sensitivity check) or a fixed cutoff (default $c = 8$, with $c \in \{6, 7, 8\}$ as sensitivity). Trimming should be applied after cross-fitted residuals are computed and before aggregating the score and variance components. Reporting requirement: always report the trimming rule, threshold, and fraction trimmed, and state whether $\hat{\theta}$ and its SE change materially under a more aggressive cutoff. A table note template is: "Residualized-treatment trimming: rule=quantile 0.995 (cutoff $c = \cdot$); trimmed x% of (i, t); estimates stable within y SEs under $Q_{0.999}$ (or $c = 6$)."

5 Asymptotic Theory

This section states high-level results for the cross-fitted DML estimator $\hat{\theta}$ defined in (6). The goal is to justify asymptotic normality and feasible inference under panel dependence, leveraging Neyman orthogonality and the product-rate condition in Assumption 6. Proofs are deferred to the Appendix. Our formal results are stated for large-N, large-T panels with time-block separation (buffer $B_T \to \infty$); when W_{it} includes within-demeaned lagged outcomes, we additionally require $\sqrt{N}/T \to 0$ to make Nickell-type contamination negligible for $\sqrt{N}$ inference (Assumption 4). Section 6 reports (i) a deliberately hard short-T stress test ($T = 8$), where additional buffering is largely infeasible and

the theory is not intended to be sharp, and (ii) a T-varying scaling experiment (Appendix A.6) that directly exercises the large-T asymptotic regime.

5.1 Setup

Let $L_* := \max\{L_y, L_d, L_x\}$ denote the maximum lag depth used in W_{it} (assumed fixed), and let $\mathcal{T}_{\text{use}} := \{L_* + 1, \dots, T\}$ denote the usable time index set (so that all lagged histories entering W_{it} exist). Let $n := N(T - L_*)$ be the effective sample size (Definition 1). Let $\eta_0 = (\ell_0, m_0)$ denote the true nuisance functions and $\hat{\eta}$ the cross-fitted estimators.

Notation for blocked-time folds with buffer. Following Algorithm 1, we partition the usable time index set $\mathcal{T}_{\text{use}}$ into K contiguous blocks $\{\mathcal{T}_k\}_{k=1}^K$. Define an *effective* buffer $B_* := B + L_*$ that both (i) separates training and test blocks by B periods for dependence control and (ii) purges training observations whose lagged feature windows would overlap the held-out test block. For an effective buffer length $B_* \geq 0$, define for each fold k:

- Test time indices: $\mathcal{T}_k$ (the k-th time block).
- Buffer time indices: $\mathcal{G}_k(B_*) := \{t \in \mathcal{T}_{\text{use}} : \min_{s \in \mathcal{T}_k} |t - s| \leq B_*\} \setminus \mathcal{T}_k$.
- Training time indices: $\mathcal{J}_k(B_*) := \mathcal{T}_{\text{use}} \setminus (\mathcal{T}_k \cup \mathcal{G}_k(B_*))$.

The fold k test set is $\mathcal{I}_k := \{(i,t) : i = 1, \dots, N; t \in \mathcal{T}_k\}$, and the fold k training set is $\mathcal{J}_k := \{(i,t) : i = 1, \dots, N; t \in \mathcal{J}_k(B_*)\}$. Nuisance functions are trained on $\mathcal{J}_k$ and scores are evaluated on $\mathcal{I}_k$ (not on the buffer $\mathcal{G}_k(B_*)$). Define the orthogonal score $\psi(\cdot, \theta, \eta)$ in (5) and the moment function

$$M(\theta, \eta) := \mathbb{E}\big[\psi(\cdot, \theta, \eta)\big].$$

Let $J_0 := \partial_\theta M(\theta, \eta_0)\big|_{\theta=\theta_0}$ denote the population Jacobian. In our setting,

$$J_0 = -\,\mathbb{E}\Big[\tilde{D}_{it}^2\Big],$$

where $\tilde{D}_{it} = \ddot{D}_{it} - m_0(W_{it})$.

5.2 Asymptotic linearity and normality

Assumption 7 (Regularity for the orthogonal score)**.** (i) $0 < \mathbb{E}[\tilde{D}_{it}^2] < \infty$ and $\mathbb{E}[\tilde{D}_{it}^4] < \infty$.

(ii) The score is Neyman-orthogonal at (θ_0, η_0) and Lipschitz in η in a neighborhood of η_0 under L_2 norms.

(iii) The cross-fitted nuisance estimators satisfy Assumption 6, and the blocked-time fold construction with effective buffer $B_{T,*} := B_T + L_*$ (Algorithm 1) yields asymptotically negligible train–test dependence under the weak serial dependence conditions in Assumption 2. Specifically, the buffer separation between the training sets $\mathcal{J}_k(B_{T,*})$ and the held-out test block $\mathcal{T}_k$ ensures

that the nuisance estimators used to score fold k are trained on observations far in time from the evaluation sample. Under the mixing conditions and the requirement that $\alpha(B_T) \to 0$ (and hence $\alpha(B_{T,*}) \to 0$ when L_* is fixed), this makes train–test dependence asymptotically negligible.

Theorem 1 (Asymptotic normality of $\hat{\theta}$)**.** *Suppose Assumptions 1, 2, 3, 5, 6, and 7 hold. Let $\hat{\theta}$ be the blocked-time cross-fitted DML estimator with effective buffer $B_{T,*} := B_T + L_*$ defined in Algorithm 1 (Section 4), where nuisances are trained on $\mathcal{J}_k(B_{T,*})$ and scores are evaluated on $\mathcal{T}_k$ for each fold $k = 1, \ldots, K$. Define the influence function at the observation level:*

$$\varphi_{it} := -J_0^{-1}\, \psi\big((Y_{it}, D_{it}, X_{it}), \theta_0, \eta_0\big),$$

where ψ is defined in (5) and $J_0 = -\mathbb{E}[\tilde{D}_{it}^2]$. Define the cluster-level influence function:

$$S_i := \frac{1}{T - L_*} \sum_{t \in \mathcal{T}_{\text{use}}} \varphi_{it}.$$

Then, as $N \to \infty$ (with T satisfying Assumption 1),

$$\sqrt{N}\,(\hat{\theta} - \theta_0) = \frac{1}{\sqrt{N}} \sum_{i=1}^{N} S_i + o_p(1),$$

and

$$\sqrt{N}\,(\hat{\theta} - \theta_0) \;\Rightarrow\; \mathcal{N}(0, \Omega),$$

where

$$\Omega := \mathrm{Var}(S_i) = \frac{1}{(T - L_*)^2} \mathrm{Var}\left(\sum_{t \in \mathcal{T}_{\text{use}}} \varphi_{it} \right)$$

under unit-level clustering (i.e., independence across i with within-i serial dependence allowed by Assumption 2).

Corollary 1 (Nickell-type contamination is $o(N^{-1/2})$ under $\sqrt{N}/T \to 0$)**.** *Suppose Assumptions 1, 2, 5, 6, 7, and 4 hold. Then the population score at θ_0 satisfies $M(\theta_0, \eta_0) = O(T^{-1})$, so the expansion in Theorem 1 becomes*

$$\sqrt{N}\,(\hat{\theta} - \theta_0) = \frac{1}{\sqrt{N}} \sum_{i=1}^{N} S_i + o_p(1) + O\left(\frac{\sqrt{N}}{T}\right).$$

In particular, if $\sqrt{N}/T \to 0$, the conclusion of Theorem 1 continues to hold with the same limiting distribution.

Remark 4 (Interpretation). The theorem states that orthogonality and blocked-time cross-fitting with buffer deliver an estimator whose first-order behavior is the same as if the nuisance functions were known. The product-rate condition $\delta_{Y,n}\delta_{D,n} = o(n^{-1/2})$ ensures that nuisance estimation error enters only at second order, despite potentially slow individual nuisance convergence rates.

The blocked-time fold construction with effective buffer $B_{T,*} = B_T + L_*$ ensures that training sets $\mathcal{J}_k(B_{T,*})$ and test sets $\mathcal{T}_k$ are separated in time *and* that no training observation's lagged feature window overlaps the held-out test block, making train–test dependence for the cross-fitted score asymptotically negligible under weak serial dependence and the condition that $\alpha(B_T) \to 0$.

Remark 5 (Role of T in the asymptotic variance). The cluster-level influence function $S_i = (T - L_*)^{-1} \sum_{t \in \mathcal{T}_{\text{use}}} \varphi_{it}$ averages the observation-level influence functions φ_{it} over the $T - L_*$ usable time periods per unit. The asymptotic variance $\Omega = \text{Var}(S_i) = (T - L_*)^{-2}\text{Var}(\sum_{t \in \mathcal{T}_{\text{use}}} \varphi_{it})$ depends on T through two channels: (i) the averaging factor $(T - L_*)^{-2}$ that scales down the variance of the sum, and (ii) the within-unit correlation structure in $\text{Var}(\sum_{t \in \mathcal{T}_{\text{use}}} \varphi_{it})$, which captures the serial dependence of the score contributions within each unit. Under weak serial dependence (Assumption 2), $\text{Var}(\sum_{t \in \mathcal{T}_{\text{use}}} \varphi_{it})$ grows on the order of T (up to long-run variance adjustments), so $\text{Var}(S_i)$ scales like $1/T$ through the $(T - L_*)^{-2}$ factor. The $\sqrt{N}$ scaling in the CLT reflects that inference is conducted at the unit (cluster) level, with T entering the variance through the within-unit aggregation. Equivalently, since $\text{Var}(\hat{\theta} - \theta_0) \approx \Omega/N$ and typically $\Omega = O(1/T)$, we have $\text{Var}(\hat{\theta} - \theta_0) = O(1/(NT))$ under weak dependence.

Proof roadmap. The proof proceeds in four steps: (i) *Orthogonal expansion*: use Neyman orthogonality to show that the moment condition error decomposes into an empirical process term and a second-order nuisance remainder; (ii) *Control of remainder terms*: the product-rate condition $\delta_{Y,n}\delta_{D,n} = o(n^{-1/2})$ implies the nuisance remainder in the sample moment is $o_p(n^{-1/2})$, so under $\sqrt{N}$ scaling it is $\sqrt{N} \cdot o_p(n^{-1/2}) = o_p(\sqrt{N/n}) = o_p((T - L_*)^{-1/2}) = o_p(1)$; (iii) *Cross-fitting and dependence*: the blocked-time fold construction with buffer B_T makes train–test dependence negligible, so cross-fitted scores behave like evaluations of a fixed score on the held-out blocks under the mixing conditions in Assumption 2 and the requirement that $\alpha(B_T) \to 0$; (iv) *Cluster CLT*: apply a cluster central limit theorem to the cluster-level influence functions S_i, leveraging independence across i and weak dependence within i to obtain asymptotic normality with $\sqrt{N}$ scaling. See the Appendix for details.

5.3 Feasible variance estimation

The variance estimator matches the implementation in Algorithm 1. Define the cross-fitted score contributions at $\hat{\theta}$:

$$\hat{\psi}_{it} := \hat{\tilde{D}}_{it}\Big(\hat{\tilde{Y}}_{it} - \hat{\theta}\,\hat{\tilde{D}}_{it}\Big),$$

where $\hat{\tilde{Y}}_{it}$ and $\hat{\tilde{D}}_{it}$ are the cross-fitted residuals from Algorithm 1. Define the cluster sums (aggregating within each unit i):

$$\hat{\Psi}_i := \sum_{t \in \mathcal{T}_{\text{use}}} \hat{\psi}_{it}.$$

The Jacobian estimator is

$$\hat{J} := -\frac{1}{n} \sum_{(i,t) \in \mathcal{I}} \hat{\tilde{D}}_{it}^2,$$

where $n = N(T - L_*)$ is the effective sample size. The unit-clustered variance estimator is

$$\hat{V} = \hat{J}^{-2} \cdot \frac{1}{n^2} \sum_{i=1}^{N} \hat{\Psi}_i^2 = \hat{J}^{-2} \cdot \frac{1}{n^2} \sum_{i=1}^{N} \left(\sum_{t \in \mathcal{T}_{\text{use}}} \hat{\psi}_{it} \right)^2 . \tag{7}$$

Theorem 2 (Consistency of $\hat{V}$)**.** *Under the conditions of Theorem 1 and mild additional moment conditions, the unit-clustered variance estimator $\hat{V}$ defined in (7) (computed using the cross-fitted estimator with buffer B_T) satisfies*

$$\hat{V} \xrightarrow{p} \frac{\Omega}{N},$$

where $\Omega = \mathrm{Var}(S_i)$ is the asymptotic variance in Theorem 1. Note that $\hat{V}$ estimates the variance of $\hat{\theta} - \theta_0$ (not the variance of $\sqrt{N}(\hat{\theta} - \theta_0)$), so $\hat{V} = O_p(N^{-1})$ and Ω/N is the limiting variance of $\hat{\theta} - \theta_0$. Consequently,

$$\frac{\hat{\theta} - \theta_0}{\sqrt{\hat{V}}} \;\Rightarrow\; \mathcal{N}(0, 1),$$

and Wald confidence intervals based on $\hat{V}$ are asymptotically valid.

5.4 Notes on dependence and fold construction

Theorems 1–2 are stated under cross-sectional independence and weak within-unit serial dependence (Assumption 2), with the blocked-time cross-fitting scheme with buffer B_T specified in Algorithm 1. The unit-clustered variance estimator accounts for within-unit serial correlation by aggregating score contributions within each unit before squaring. In applications with strong common time shocks, one could alternatively use time-clustered or two-way clustered variance estimators, though the theory for such extensions is not developed here. The key requirement for cross-fitting is that the fold design with buffer B_T yields asymptotically negligible train–test dependence under the mixing conditions in Assumption 2 and the requirement that $\alpha(B_T) \to 0$.

6 Simulation Study

This section evaluates the finite-sample performance of the proposed blocked-time DML estimator across a full grid of dependence, dimensionality, and confounding scenarios. We compare four estimators that differ in orthogonality and sample splitting to isolate when those design choices matter for bias and inference.

6.1 Simulation Design

We simulate balanced panels with $N = 200$ units and $T = 8$ periods as a deliberately hard short-T stress test. The main theoretical results in Section 5 are stated for moderately large/growing T with time-block separation, so this short-T design is not meant to "validate" the asymptotics; it is meant to show what breaks first when T is too small to support aggressive fold purging/buffering.

The target parameter is $\theta_0 = 1.0$, representing the structural treatment effect in the partially linear dynamic panel model described in Section 3. For each unit i, an unobserved fixed effect α_i is drawn once from a standard normal distribution and remains constant across time periods.

The data-generating process follows:

$$Y_{it} = \rho Y_{i,t-1} + \theta_0 D_{it} + g(X_{it}) + \alpha_i + U_{it}, \tag{8}$$

$$D_{it} = h(X_{it}) + 0.3 Y_{i,t-1} + \gamma \alpha_i + V_{it}, \tag{9}$$

where (U_{it}, V_{it}) are i.i.d. standard normal errors, and the functions $g(\cdot)$ and $h(\cdot)$ control the strength and form of confounding. All estimators remove α_i using the global within transformation (demeaning by unit over all $t = 1, \ldots, T$), consistent with Algorithm 1; the fold-specific within-demeaning variant in Section 4 is not used in the reported simulation tables unless stated otherwise.

The grid varies:

- **Serial dependence** $\rho \in \{0.0, 0.4, 0.5, 0.8\}$
- **Dimensionality** $p \in \{50, 200\}$
- **Confounding structure**: nonlinear vs. linear $g(\cdot)$ and $h(\cdot)$, and confounding strength $\gamma \in \{1.0, 2.0\}$

In nonlinear scenarios, $g(x) = 0.6 \sin(z_1) + 0.2 z_2$ and $h(x) = 0.8 \tanh(z_1) + 0.3 z_2^2$, where $z_1 = x'b/\sqrt{p}$ and $z_2 = x'c/\sqrt{p}$ for random coefficient vectors (b, c). We also report a stress-test variant that adds thresholded interactions and higher-frequency components in $g(\cdot)$ and $h(\cdot)$ to induce learner mismatch. In linear scenarios, $g(\cdot)$ and $h(\cdot)$ are linear functions of the first few covariates.

All estimators use blocked-time cross-fitting with $K = 4$ folds (when applicable), where folds are constructed by splitting time periods into contiguous blocks. Because $T = 8$ leaves little room for additional separation beyond the lag purge built into Algorithm 1, we set the additional buffer parameter to $B = 0$ in the main grid. This does *not* mean folds are unpurged: with lagged features, $B = 0$ still implies an effective buffer of $B_* = L_*$ (Algorithm 1). We emphasize that $B = 0$ is a short-T stress-test/heuristic setting used here because growing buffers (e.g., $B = \lceil \log T \rceil$) would remove too much data when $T = 8$. For theory-aligned evidence, Appendix A.6 varies T and uses buffer sequences B_T that grow with T (e.g., $B_T = \lceil \log T \rceil$), directly exercising the asymptotic regime in Assumption 1. We report $R = 200$ Monte Carlo replications. We also evaluate buffer sensitivity at $B \in \{0, 1, 2\}$ for the high-dependence/high-confounding scenario ($\rho = 0.8$, $p = 50$, nonlinear, $\gamma = 2.0$).

6.2 Estimators Compared

We compare four estimators that isolate the value of orthogonality and cross-fitting:

- **FE-OLS (baseline)**: Linear fixed-effects OLS with $(Y_{i,t-1}, D_{it}, X_{it})$ entering linearly.

- **Post-ML (non-orthogonal)**: Lasso post-selection OLS for $Y \sim D + W$, or RF residualization $Y - \hat{Y}(W)$ on D.
- **Orthogonal-no-split**: Partialling-out with nuisances trained on the full sample (no splitting).
- **DML (blocked-time cross-fitting)**: Algorithm 1 in Section 4 with $K = 4$ folds and unit-clustered standard errors.

6.3 Performance Metrics

For each method and scenario, we report bias, RMSE, empirical SD, mean SE, coverage, and size. Coverage and size are computed using unit-clustered robust standard errors, consistent with Section 5.

6.4 Main Results

Table 2 reports bias, RMSE, and coverage for the full grid; Table 3 reports coverage with Monte Carlo standard errors (MCSE). The detailed metrics (bias, RMSE, empirical SD, mean SE, size) are reported in Appendix Table 8.

Table 2: Monte Carlo results across scenarios: bias, RMSE, and coverage of nominal 95% confidence intervals. Scenarios vary serial dependence (ρ), dimensionality (p), and confounding structure (nonlinear vs. linear, strong vs. moderate).

	FE-OLS			Post-ML (Lasso)			Orthogonal-no-split (Lasso)			DML (Lasso)		
Scenario	Bias	RMSE	Cov.	Bias	RMSE	Cov.	Bias	RMSE	Cov.	Bias	RMSE	Cov.
rho=0.0, p=50, nonlinear	0.002	0.028	0.94	0.003	0.028	0.94	0.000	0.028	0.94	0.008	0.030	0.91
rho=0.5, p=50, nonlinear	-0.009	0.029	0.92	-0.008	0.029	0.92	-0.011	0.030	0.91	0.005	0.030	0.90
rho=0.8, p=50, nonlinear	-0.004	0.029	0.95	-0.002	0.029	0.94	-0.003	0.029	0.94	0.008	0.032	0.89
rho=0.4, p=200, nonlinear	-0.012	0.032	0.94	0.021	0.041	0.81	-0.028	0.046	0.74	0.015	0.037	0.86
rho=0.4, p=50, linear	-0.031	0.042	0.80	-0.032	0.044	0.77	-0.032	0.043	0.77	-0.018	0.035	0.90
rho=0.4, p=50, strong confound	0.004	0.023	0.95	0.009	0.027	0.91	0.004	0.023	0.96	0.012	0.026	0.90

Notes: Entries show bias, RMSE, and coverage over $R = 200$ replications. All methods use unit-clustered robust standard errors. DML uses blocked-time cross-fitting with $K = 4$ folds. Coverage marked as "–" indicates standard errors were not available or invalid.

Two patterns are most salient. First, inference without orthogonality and/or sample splitting can under-cover in high-dimensional nonlinear settings: for $\rho = 0.4$, $p = 200$, nonlinear, Post-ML coverage is 0.81 and Orthogonal-no-split coverage is 0.74, while DML coverage is 0.86. Second, in moderate linear settings, orthogonality and cross-fitting improve coverage: for $\rho = 0.4$, $p = 50$, linear, $\gamma = 1.0$, DML coverage is 0.90 versus 0.77 for Post-ML and 0.80 for FE-OLS. Bias and RMSE follow a similar pattern in difficult regimes: in the high-dimensional nonlinear case ($\rho = 0.4$, $p = 200$), DML bias/RMSE are 0.015 and 0.037 versus 0.021 and 0.041 for Post-ML (and -0.028 and 0.046 for Orthogonal-no-split). DML is not uniformly dominant: in easier designs without strong confounding (e.g., $\rho = 0.0$, $p = 50$, nonlinear), FE-OLS coverage is 0.94 while DML coverage is 0.91, reflecting the efficiency cost of sample splitting when the nuisance structure is simple.

Table 3: Coverage with Monte Carlo standard errors (MCSE) for nominal 95% confidence intervals. MCSE computed as $\sqrt{\text{coverage} \times (1 - \text{coverage})/R}$ where $R = 200$.

Scenario	FE-OLS	Post-ML (Lasso)	Orthogonal-no-split (Lasso)	DML (Lasso)
rho=0.0, p=50, nonlinear	0.94 (0.02)	0.94 (0.02)	0.94 (0.02)	0.91 (0.02)
rho=0.5, p=50, nonlinear	0.92 (0.02)	0.92 (0.02)	0.91 (0.02)	0.90 (0.02)
rho=0.8, p=50, nonlinear	0.95 (0.01)	0.94 (0.02)	0.94 (0.02)	0.89 (0.02)
rho=0.4, p=200, nonlinear	0.94 (0.02)	0.81 (0.03)	0.74 (0.03)	0.86 (0.02)
rho=0.4, p=50, linear	0.80 (0.03)	0.77 (0.03)	0.77 (0.03)	0.90 (0.02)
rho=0.4, p=50, strong confound	0.95 (0.01)	0.91 (0.02)	0.96 (0.01)	0.90 (0.02)

Notes: Entries show coverage (MCSE in parentheses). MCSE quantifies simulation uncertainty in coverage estimates.

6.5 Coverage and Diagnostics

Figure 1 plots coverage across the grid, and Figure 2 summarizes bias and RMSE. Appendix Table 9 reports SE ratios (mean reported SE divided by empirical SD). In high-dimensional nonlinear settings, SE ratios indicate underestimation for non-orthogonal methods; for $\rho = 0.4$, $p = 200$, nonlinear, the Post-ML SE ratio is 0.74 while DML is 0.80.

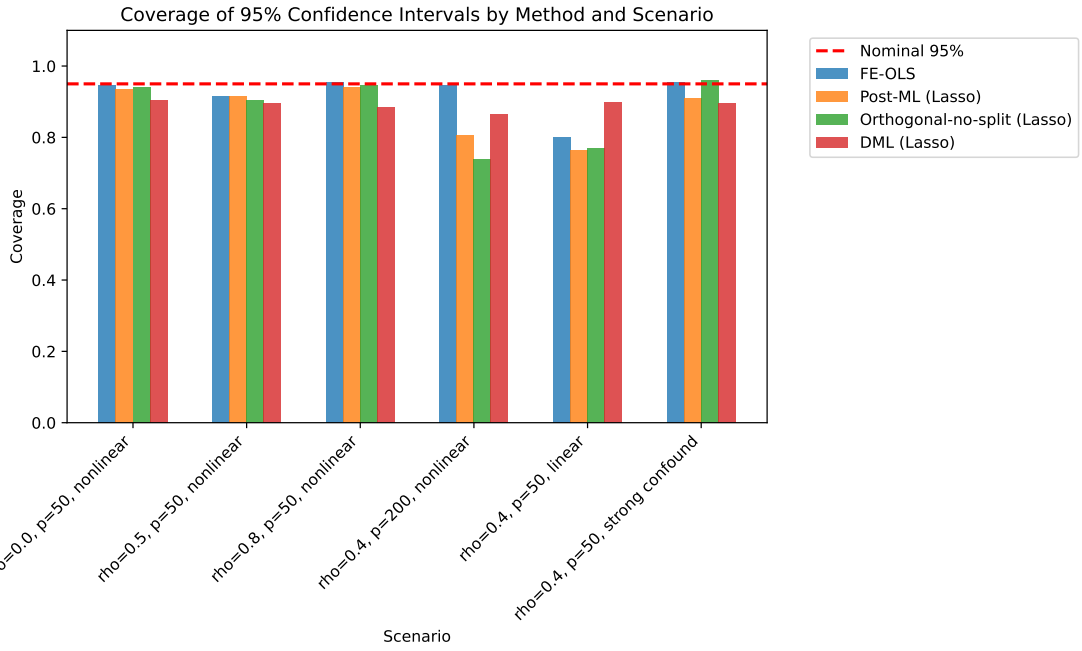

Figure 1: Empirical coverage of nominal 95% confidence intervals by method and scenario. The horizontal dashed line indicates the nominal 95% level.

The stress-test highlights a practical lesson: orthogonal scores mitigate first-order bias, but poor nuisance fits can still leave meaningful bias and undercoverage in very short-T settings. Flexible learners (RF, GBM) improve performance relative to Lasso under the stress DGP, but do not fully eliminate distortions, underscoring the value of comparing learners and monitoring nuisance fit diagnostics in applied work.

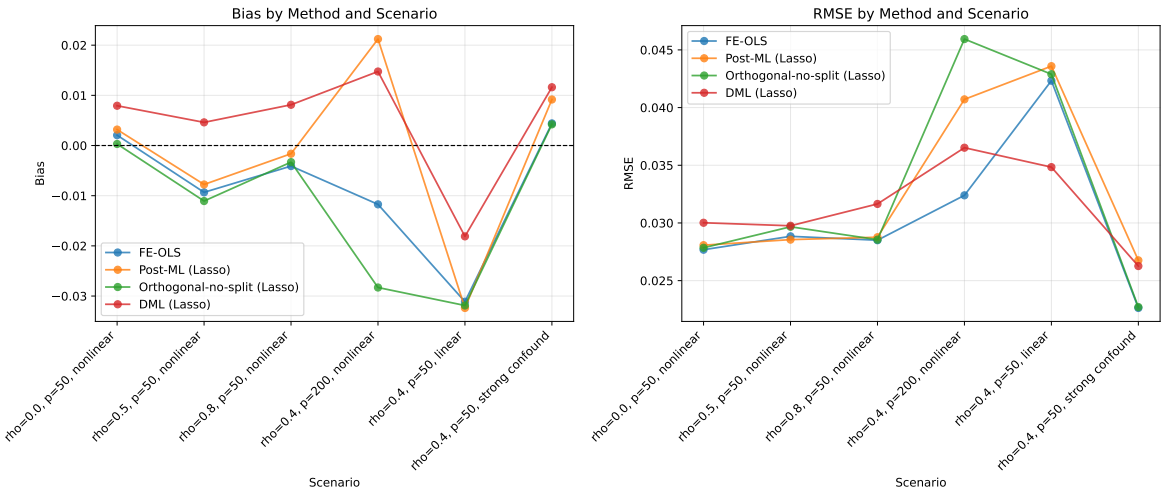

Figure 2: Bias and RMSE by method and scenario. Left panel shows bias (deviation from true $\theta_0 = 1.0$); right panel shows RMSE.

6.6 Failure Mode: When DML Does Not Save You

The scaling experiment in Appendix A.6 makes the boundary conditions explicit. As T grows in the nonlinear DGP with a linear learner, coverage can collapse even though standard errors tighten: bias does not shrink with T, so t-statistics drift and coverage falls. This pattern indicates nuisance misspecification rather than a variance-scaling bug. The main lesson is crisp: orthogonality removes first-order sensitivity, but the product-rate conditions are still substantive and can fail when the nuisance learner class is misspecified. In that case, DML does not rescue inference; stronger or better-specified nuisance learning is required. Figure 4 summarizes coverage versus T under growing-buffer rules; Appendix A.6 reports the corresponding tables and extended diagnostics.

6.7 Buffer Sensitivity

Table 4 reports the buffer sensitivity experiment for $\rho = 0.8$, $p = 50$, nonlinear, $\gamma = 2.0$ using DML with Lasso. Coverage declines from 0.78 at $B = 0$ to 0.67 at $B = 1$ and 0.61 at $B = 2$, reflecting the loss of effective training data at $T = 8$ when buffer gaps remove two time blocks per fold. This is a short-T tradeoff, not a general recommendation: with $T = 8$, adding buffer periods can starve the nuisance learners, so enforcing more separation can reduce coverage even though it improves fold purity. In moderate/large T panels, additional buffers are feasible and are part of the asymptotic guardrails (Section 5); Appendix A.6 illustrates that regime.

6.8 Empirical Validation

This exercise is a sanity check: it demonstrates that the blocked-time cross-fitting and clustered-inference pipeline runs end-to-end on a real macro panel, and it motivates the standardized-shock scaling when raw units are unclear. The robustness grid across outcomes, lags, buffers, and learners

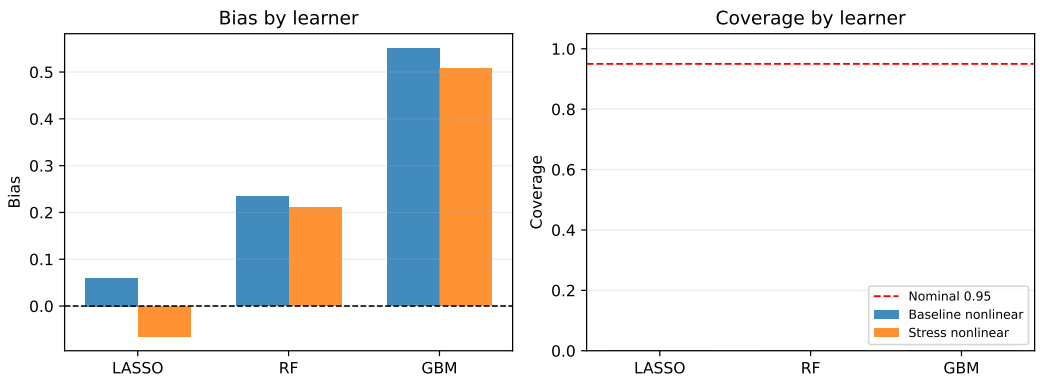

Figure 3: Nuisance misspecification stress test. DML with blocked-time cross-fitting is evaluated under baseline nonlinear vs. stress nonlinear confounding. The stress DGP introduces thresholded interactions that challenge linear nuisance models.

is presented as specification discipline rather than a search for a single headline magnitude.

We validate the estimator on a quarterly panel combining GMD macroeconomic outcomes with IMF monetary policy shocks. The treatment is the IMF shock series `mps` from `MP_shocks_11172025.csv`, and outcomes are GDP measures in log differences (diff_log), interpreted as growth rates. The sample spans $N = 20$ countries over $T = 90$ quarters (2000–2022); after lag construction and missingness the panel is mildly unbalanced, with $n = 1444$ usable country–quarter observations for the baseline specification. Because the raw unit of `mps` is not documented in the file headers, we report both raw-unit estimates and a standardized-shock scaling (specification S6), where coefficients can be read as effects per 1 standard deviation of the shock in the estimation sample. We estimate the blocked-time DML estimator with $K = 4$ folds, a theory-aligned baseline buffer $B = \lceil \log T \rceil$ (here $B = 5$), and lags $(y\_lags, x\_lags) = (1, 1)$; we report $B = 0$ (lag purge only) as a heuristic stress test and vary outcomes, lags, buffers, and learners.

In the standardized-shock specification (S6), a one-standard-deviation increase in the IMF shock is associated with $\hat{\theta} = 2.69 \times 10^{-3}$ (SE 1.23×10^{-3}, t-stat 2.19) for quarterly diff_log `ngdp`. The standard deviation used for standardization is 26.45 in the estimation sample. Across the robustness grid, estimates remain small in magnitude and include sign changes across learners.

This macro panel is a reasonable sanity check for the estimator because it sits in a regime where blocked-time cross-fitting with buffers is feasible ($T = 90$), and it features serial dependence, high-dimensional controls, and potentially nonlinear confounding in policy transmission. The blocked-time cross-fitting design and unit-clustered inference are meant to be robust to within-country dependence and overfitting in the nuisance regressions; this setting directly exercises those mechanisms.

At the same time, the exercise is not a definitive causal claim about monetary policy and it is not covered by the cross-sectional independence assumptions used in the main theorems if common time shocks induce residual cross-country dependence. The goal is to show that, in a realistic macro panel with a plausibly exogenous shock series and rich controls, the estimator yields stable

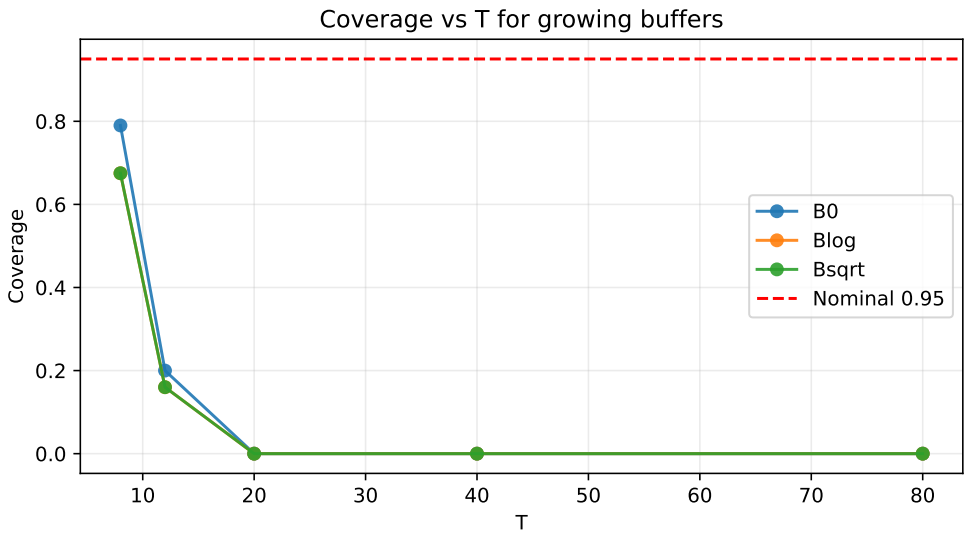

Figure 4: Coverage versus T for growing buffer rules in the scaling experiment (Appendix A.6).

inference that is not mechanically driven by the choice of learner, buffer, or lag structure. Small and unstable estimates across specifications are consistent with a limited-signal environment and highlight the importance of strong nuisance learning rather than providing a headline effect.

6.9 Relation to Legacy Single-Scenario Results

Table 7 and Figure 5 report results from a simpler single-scenario design ($\rho = 0.4$, $p = 20$, $R = 60$) used in earlier versions of this paper.

The legacy results are qualitatively consistent with the expanded grid: naive plug-in approaches show modest bias, while cross-fitted DML estimators reduce bias and improve coverage in the difficult scenarios.

6.10 Reproducibility Note

The simulation runner records a run manifest (including seeds, configuration, and package versions) under `outputs/simulations/runs/`. The empirical validation grid writes an analogous manifest under `outputs/empirical_validation/runs/`. These manifests document the exact configuration used to produce the tables and figures included in this section.

7 Conclusion

This paper addresses a gap in inference for dynamic target parameters in panel data with high-dimensional controls: standard double machine learning methods assume i.i.d. observations, while dynamic panels exhibit serial dependence and fixed effects; classical dynamic panel inference is not designed for machine-learning-based nuisance estimation, which can introduce regularization

Table 4: Buffer sensitivity for DML (Lasso) in the high-dependence/high-confounding scenario ($\rho = 0.8$, $p = 50$, nonlinear, $\gamma = 2.0$). Results over $R = 200$ replications.

B	Bias	RMSE	Coverage
0	0.024	0.035	0.78
1	0.029	0.040	0.67
2	0.033	0.045	0.61

Notes: B is the *additional* separation buffer in Algorithm 1; with lagged features, the effective buffer is $B_* = B + L_*$.

Table 5: Empirical validation baseline specification. The outcome is diff_log `ngdp`, and the treatment is `mps`.

Spec	Outcome	$\dot{\theta}$ (SE)	n	Countries	Periods	Learner	K	Buffer	Lags (y/x/d_W)
S0	ngdp	1.43×10^{-4} (6.91×10^{-5})	1444	20	89	lasso	4	5	1/1/1

Notes: n is the number of usable unit–time observations (after lag construction and missingness). Lags (y/x/d_W) denote outcome, control, and treatment-history lags included in W_{it}. Blocked-time cross-fitting with unit fixed effects and unit-clustered standard errors. In macro panels, residual common time shocks can induce cross-sectional dependence not covered by the baseline theory; consider time fixed effects and/or time/two-way clustered inference as robustness.

and overfitting biases. We address this gap by combining orthogonal score construction with dependence-aware cross-fitting, delivering an estimator that reduces regularization bias and overfitting in machine-learned nuisance components while respecting the panel structure through blocked-time folds and unit-clustered variance estimation.

7.1 Theoretical Contribution

Our theoretical results establish asymptotic normality of the cross-fitted DML estimator under a large-N panel asymptotic framework with weak within-unit serial dependence (specifically, α-mixing with summable coefficients) and cross-sectional independence. The key technical contributions are: (i) an orthogonal score construction that decouples target inference from nuisance estimation error, ensuring that nuisance estimation error enters only at second order under a product-rate condition; (ii) a blocked-time cross-fitting scheme that respects serial dependence by holding out contiguous blocks of time periods across all units, ensuring that training and test sets are separated in time and that train–test dependence in the cross-fitted scores is asymptotically negligible under the mixing conditions; and (iii) a unit-clustered variance estimator that accounts for within-unit serial correlation by aggregating score contributions within each unit before squaring, delivering feasible inference with $\sqrt{N}$ scaling. The results hold under high-level rate conditions

Table 6: Empirical robustness grid across outcomes, lags, buffer periods, and learners.

Spec	Outcome	$\hat{\theta}$ (SE)	n	Countries	Periods	Learner	K	Buffer	Lags (y/x/d_W)
S0_base	ngdp	1.43×10^{-4} (6.91×10^{-5})	1444	20	89	lasso	4	5	1/1/1
S1_alt_outcome	ngdp_usd	8.72×10^{-5} (6.36×10^{-5})	1444	20	89	lasso	4	5	1/1/1
S2_lags_2	ngdp	7.40×10^{-6} (3.77×10^{-5})	1424	20	88	lasso	4	5	2/2/1
S3_buffer_0	ngdp	1.09×10^{-4} (5.09×10^{-5})	1444	20	89	lasso	4	0	1/1/1
S4_learner_ridge	ngdp	1.57×10^{-4} (8.33×10^{-5})	1444	20	89	ridge	4	5	1/1/1
S5_alt_outcome_ridge	ngdp_usd	1.40×10^{-4} (1.14×10^{-4})	1444	20	89	ridge	4	5	1/1/1
S6_std_mps_base	ngdp	2.69×10^{-3} (1.23×10^{-3})	1444	20	89	lasso	4	5	1/1/1
S7_std_mps_ridge	ngdp	4.16×10^{-3} (2.20×10^{-3})	1444	20	89	ridge	4	5	1/1/1
S8_winsor_1pct_base	ngdp	7.63×10^{-5} (9.96×10^{-5})	1444	20	89	lasso	4	5	1/1/1
S9_winsor_1pct_std_base	ngdp	1.04×10^{-3} (1.25×10^{-3})	1444	20	89	lasso	4	5	1/1/1

Notes: n is the number of usable unit–time observations (after lag construction and missingness). Lags (y/x/d_W) denote outcome, control, and treatment-history lags included in W_{it}. Blocked-time cross-fitting with unit fixed effects and unit-clustered standard errors. In macro panels, residual common time shocks can induce cross-sectional dependence not covered by the baseline theory; consider time fixed effects and/or time/two-way clustered inference as robustness.

Table 7: Monte Carlo summary for θ_0 in a nonlinear dynamic panel (legacy single-scenario design: $\rho = 0.4$, $p = 20$, $R = 60$).

	mean	sd	bias	rmse
FE-OLS (linear controls)	0.996	0.024	-0.004	0.024
Naive plug-in (Lasso, no split)	0.996	0.024	-0.004	0.024
DML (Lasso, blocked-time)	1.004	0.027	0.004	0.027
DML (RF, blocked-time)	1.059	0.028	0.059	0.065

Notes: Entries report the Monte Carlo mean, standard deviation (sd), bias, and RMSE over $R = 60$ replications. DML uses blocked-time cross-fitting with $K = 4$ folds and unit-clustered standard errors.

on the nuisance learners, allowing for flexible ML methods such as Lasso or random forests, and require T to be sufficiently large relative to the number of folds K; when W_{it} includes within-demeaned lagged outcomes, we additionally require $\sqrt{N}/T \to 0$ so Nickell-type contamination is $o(N^{-1/2})$ for inference on θ_0 (Assumption 4).

7.2 Simulation Evidence

The Monte Carlo evidence in Section 6 supports the theoretical predictions and clarifies when the benefits of orthogonality and cross-fitting are most material. Table 2 reports bias, RMSE, and coverage across six scenarios that vary serial dependence (ρ), dimensionality (p), and confounding structure. Figure 1 plots empirical coverage of 95% confidence intervals, and Figure 2 shows bias and RMSE patterns.

Several robust patterns emerge. (i) **DML improves inference reliability in challenging scenarios.** In high-dimensional settings ($p = 200$, $\rho = 0.4$, nonlinear), DML achieves coverage of 0.86 while Orthogonal-no-split drops to 0.74, and DML shows lower bias (0.015) than Orthogonal-no-split (-0.028). Under strong serial dependence ($\rho = 0.8$), DML coverage is 0.89 (below nominal), while other methods achieve coverage of 0.93–0.94; DML shows slightly higher RMSE (0.032 vs 0.029) in this scenario. Across the grid, DML coverage ranges from 0.86 to 0.91, with the lowest coverage (0.86) occurring in the high-dimensional scenario and the highest (0.91) in scenarios with low to moderate serial dependence. (ii) **Orthogonal-no-split can miscover when dimensionality is high.** Without sample splitting, regularization bias accumulates in high-dimensional scenarios, leading to coverage as low as 0.74 in the $p = 200$ case, despite using orthogonal scores. (iii) **Post-ML (non-orthogonal) can exhibit bias and miscoverage.** Post-ML shows similar or slightly larger bias than orthogonal methods in most scenarios, with coverage ranging from 0.77 to 0.94. The differences are most pronounced in high-dimensional settings, where regularization

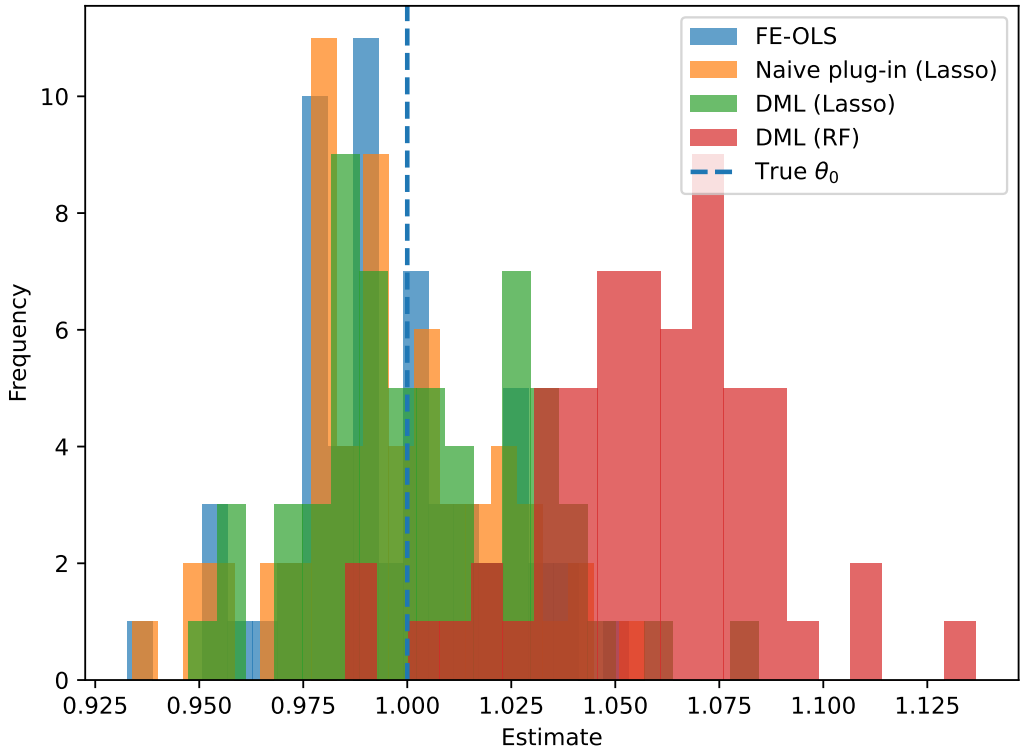

Figure 5: Sampling distributions of estimators of θ_0 across Monte Carlo replications (legacy single-scenario design: $\rho = 0.4$, $p = 20$).

bias from non-orthogonal estimation becomes material. (iv) **FE-OLS provides a useful benchmark but degrades under misspecification.** FE-OLS performs reasonably well when controls are linear (coverage 0.80), but bias can be substantial (-0.032) when the linear approximation is poor or when p is large.

These patterns align with the theoretical framework: orthogonality removes first-order bias from nuisance estimation error, while cross-fitting controls overfitting effects that can inflate variance estimates. The combination of both (DML) provides reliable inference across the scenario grid, with particular benefits in high-dimensional settings with strong confounding.

7.3 Practical Guidance

For applied researchers using DML in dynamic panel settings, we offer the following recommendations. (i) **When to prefer DML over FE-OLS:** DML is particularly valuable when the number of controls p is large relative to sample size, confounding is suspected to be nonlinear, or flexible nuisance adjustment is needed to satisfy exogeneity conditions. When p is small and controls are well-approximated by linear functions, FE-OLS may be sufficient and computationally simpler. (ii) **Fold choice:** Use blocked-time cross-fitting with K fixed (e.g., $K = 4$) and T sufficiently large relative to K (e.g., $T \geq 2K$). The blocked-time construction separates training and test sets in

time, reducing overfitting bias while maintaining compatibility with weak serial dependence under the mixing conditions. For theoretical convenience under serial dependence, Section 5 states results for a buffer length B_T that grows slowly with T (so $\alpha(B_T) \to 0$). Algorithm 1 defaults to a growing-buffer rule such as $B = \lceil \log T \rceil$ (as required by the main asymptotic framework), and allows $B = 0$ only as a short-T stress-test/heuristic setting. In very short panels, additional buffering can be infeasible and $B = 0$ should be read as "lag purge only" rather than as an endorsement of no separation. When T is moderate/large, buffers are feasible and align the fold construction with the asymptotic guardrails (Section 5); reporting sensitivity to $B > 0$ is recommended when serial dependence is strong. (iii) **Caution for short panels and highly persistent series:** When T is very small (e.g., $T < 6$), Nickell-type bias may be non-negligible, and the blocked-time fold construction may leave insufficient observations per fold. This limitation should be investigated in future work, as our simulations use $T = 8$ and do not cover very short panels. For highly persistent series (ρ near 1), consider increasing T or using alternative moment-based approaches that explicitly handle dynamic bias. Our simulations cover ρ up to 0.8; in the short-T grid (Table 2), performance does deteriorate in the $\rho = 0.8$ regime, and the buffer-sensitivity experiment (Table 4) illustrates the practical tradeoff between fold purity and nuisance-learning precision when T is small. (iv) **Learner quality diagnostics:** Monitor out-of-sample fit quality for nuisance learners (e.g., out-of-sample R^2 or MSE on held-out folds) to detect weak identification or poor nuisance estimation. If residualized treatment variance is very small, inference may be unreliable regardless of method choice. (v) **Variance estimation:** Use unit-clustered robust standard errors as implemented in Algorithm 1, which accounts for within-unit serial correlation. In settings with strong common time shocks, consider time-clustered or two-way clustered variance estimators, though the theory for such extensions is not developed here. (vi) **Learner selection:** DML is modular with respect to the ML learners, but finite-sample performance depends on tuning and validation. For time series, use blocked validation rather than naive i.i.d. cross-validation. Lasso is a natural default for high-dimensional linear confounding; random forests may help with nonlinear confounding but require careful tuning to avoid bias.

7.4 Limitations and Extensions

Several directions are promising for strengthening the framework and broadening its applicability.

Short panels and dynamic bias. When T is very small, Nickell-type bias may be non-negligible for the autoregressive coefficient and can contaminate inference if not handled carefully. A natural extension is to combine orthogonal-score DML with classical moment restrictions (e.g., Arellano–Bond/Arellano–Bover/Blundell–Bond style constructions) to obtain a bias-robust dynamic component while retaining flexible nuisance adjustment. Doing so requires careful integration of orthogonalization with instrument selection and cross-fitting, and may benefit from time buffers in finite samples to reduce leakage under strong persistence.

Cross-sectional dependence. The theory in the main text is stated under cross-sectional independence with weak within-unit serial dependence. Extending the results to panels with strong

factor structures, network dependence, or persistent aggregate shocks is important for macro-finance applications. Methodologically, this points to fold designs and variance estimators that explicitly accommodate common components, potentially using factor-augmented nuisance learning and two-way (unit×time) clustering, though the theoretical development of such extensions is beyond the scope of this paper.

Richer dynamics and heterogeneous effects. Empirically, dynamic responses can be nonlinear and heterogeneous across units and states. The orthogonal-score approach extends naturally to distributed-lag specifications, state-dependent effects, and partially linear models with interactions (e.g., θ_0 varying with a low-dimensional state variable). This would permit impulse-response style objects that remain robust to high-dimensional confounding.

Finite-sample calibration and tuning. Systematic guidance on blocked validation, hyperparameter stability, and learner choice in dynamic panels remains a valuable area for future work. The simulation evidence suggests that DML is robust across a range of scenarios, but practitioner guidance on tuning and validation in finite samples would strengthen the framework.

7.5 Takeaway

The main message is that valid inference for dynamic target parameters is feasible even in richly confounded panel settings, provided one uses orthogonal moments and cross-fitting tailored to dependence. The combination of orthogonality and blocked-time cross-fitting delivers inference that reduces regularization bias and overfitting, with coverage ranging from 0.86 to 0.91 across scenarios in this grid, showing particular benefits in high-dimensional settings with strong confounding. This template is intended to be directly usable by practitioners who want to bring modern ML flexibility to dynamic panel designs without sacrificing inferential credibility.

References

M. Arellano and S. Bond. Some tests of specification for panel data: Monte carlo evidence and an application to employment equations. *The Review of Economic Studies*, 58(2):277–297, 1991.

M. Arellano and O. Bover. Another look at the instrumental variable estimation of error-components models. *Journal of Econometrics*, 68(1):29–51, 1995.

S. Basu and G. Michailidis. Regularized estimation in sparse high-dimensional time series models. *The Annals of Statistics*, 43(4):1535–1567, 2015.

A. Belloni, V. Chernozhukov, and C. Hansen. Inference on treatment effects after selection among high-dimensional controls. *Review of Economic Studies*, 81(2):608–650, 2014.

R. Blundell and S. Bond. Initial conditions and moment restrictions in dynamic panel data models. *Journal of Econometrics*, 87(1):115–143, 1998.

V. Chernozhukov, D. Chetverikov, M. Demirer, E. Duflo, C. Hansen, W. Newey, and J. Robins. Double/debiased machine learning for treatment and structural parameters. *The Econometrics Journal*, 21(1):C1–C68, 2018.

J. Hahn and G. M. Kuersteiner. Asymptotically unbiased inference for a dynamic panel model with fixed effects when both n and t are large. *Econometrica*, 70(4):1639–1657, 2002.

S. Nickell. Biases in dynamic models with fixed effects. *Econometrica*, 49(6):1417–1426, 1981.

P. M. Robinson. Root-n-consistent semiparametric regression. *Econometrica*, 56(4):931–954, 1988.

W. B. Wu and Y. Wu. Performance bounds for parameter estimation in high-dimensional linear regression with dependent observations. *The Annals of Statistics*, 44(6):2465–2494, 2016.

A Appendix: Proofs and Additional Results

This appendix provides proof sketches for the main asymptotic results and records a joint-score extension for estimating (ρ_0, θ_0) simultaneously.

A.1 A.1 Proof sketch for Theorem 1 (asymptotic normality)

We sketch the standard DML argument adapted to unit clustering and weak within-unit dependence.

Step 1: Cross-fitted moment equation. Let $\hat{\eta}$ denote the cross-fitted nuisance estimates and define the sample moment

$$\hat{M}(\theta) := \frac{1}{n} \sum_{(i,t)\in\mathcal{I}} \psi\big((Y_{it}, D_{it}, X_{it}), \theta, \hat{\eta}\big).$$

By construction, the pooled estimator $\hat{\theta}$ in (6) solves $\hat{M}(\hat{\theta}) = 0$.

Step 2: Linearization in θ. A mean-value expansion yields

$$0 = \hat{M}(\hat{\theta}) = \hat{M}(\theta_0) + \hat{J}(\bar{\theta})\,(\hat{\theta} - \theta_0),$$

where $\hat{J}(\bar{\theta})$ is the sample Jacobian evaluated at an intermediate value $\bar{\theta}$. Under Assumption 7 and standard stability arguments, $\hat{J}(\bar{\theta}) \xrightarrow{p} J_0$ with $J_0 = -\mathbb{E}[\tilde{D}_{it}^2]$.

Step 3: Orthogonality and nuisance remainder. Decompose the centered moment:

$$\hat{M}(\theta_0) - M(\theta_0, \eta_0) = \underbrace{\Big(\hat{M}(\theta_0) - M(\theta_0, \hat{\eta})\Big)}_{\text{empirical process}} + \underbrace{\Big(M(\theta_0, \hat{\eta}) - M(\theta_0, \eta_0)\Big)}_{\text{nuisance effect}}.$$

The nuisance effect is second order because the score is Neyman-orthogonal at (θ_0, η_0) and the nuisances satisfy the product-rate condition in Assumption 6. Formally, a Taylor expansion in η plus orthogonality implies

$$M(\theta_0, \hat{\eta}) - M(\theta_0, \eta_0) = O_p(\|\hat{\ell} - \ell_0\|_2 \cdot \|\hat{m} - m_0\|_2) = o_p(n^{-1/2}).$$

Since $n = N(T - L_*)$ with fixed L_*, this remainder is negligible under $\sqrt{N}$ scaling: $\sqrt{N} \cdot o_p(n^{-1/2}) = o_p(\sqrt{N/n}) = o_p((T - L_*)^{-1/2}) = o_p(1)$. Cross-fitting ensures that the empirical process term behaves as if the nuisances were fixed (trained on an independent sample), up to negligible dependence induced by weak time dependence and fold construction.

Step 4: Cluster CLT and influence function. Combining the above, we obtain the asymptotic linear representation

$$\sqrt{N}(\hat{\theta} - \theta_0) = -J_0^{-1} \cdot \frac{1}{\sqrt{N}} \sum_{i=1}^{N} \Big(\frac{1}{T - L_*} \sum_{t \in \mathcal{T}_{\text{use}}} \psi\big((Y_{it}, D_{it}, X_{it}), \theta_0, \eta_0\big) \Big) + o_p(1).$$

Define the observation-level influence function $\varphi_{it} := -J_0^{-1} \psi((Y_{it}, D_{it}, X_{it}), \theta_0, \eta_0)$ and the cluster-level influence function $S_i := (T - L_*)^{-1} \sum_{t \in \mathcal{T}_{\text{use}}} \varphi_{it}$ as in Theorem 1. Then the representation becomes

$$\sqrt{N}(\hat{\theta} - \theta_0) = \frac{1}{\sqrt{N}} \sum_{i=1}^{N} S_i + o_p(1).$$

Under Assumption 2, the clusters $\{S_i\}_{i=1}^{N}$ are independent across i (since units are independent) and each S_i aggregates weakly dependent within-unit observations. A cluster (unit-level) central limit theorem yields asymptotic normality with variance $\Omega = \text{Var}(S_i)$ as stated in Theorem 1.

A.2 A.1.1 Proof sketch for Corollary 1 (Nickell-type contamination)

Corollary 1 relaxes the exact conditional mean restriction in Assumption 3 and allows a small (Nickell-order) violation as in Assumption 4. Write the score at the true nuisances as

$$\psi_{it}(\theta, \eta_0) = \tilde{D}_{it}\big(\tilde{Y}_{it} - \theta\, \tilde{D}_{it}\big),$$

where $\tilde{Y}_{it} = \ddot{Y}_{it} - \ell_0(W_{it})$ and $\tilde{D}_{it} = \ddot{D}_{it} - m_0(W_{it})$. Using $\ddot{Y}_{it} = \theta_0 \ddot{D}_{it} + h_0(W_{it}) + \ddot{U}_{it}$ and the definitions of (ℓ_0, m_0), we have

$$\tilde{Y}_{it} - \theta_0 \tilde{D}_{it} = \ddot{U}_{it} - \mathbb{E}[\ddot{U}_{it} \mid W_{it}].$$

Therefore the population moment at θ_0 satisfies

$$M(\theta_0, \eta_0) = \mathbb{E}[\psi_{it}(\theta_0, \eta_0)] = \mathbb{E}[\tilde{D}_{it} \ddot{U}_{it}],$$

since $\mathbb{E}[\tilde{D}_{it}\mathbb{E}[\ddot{U}_{it} \mid W_{it}]] = 0$ by $\mathbb{E}[\tilde{D}_{it} \mid W_{it}] = 0$. Under Assumption 4, $\mathbb{E}[\ddot{U}_{it} \mid \ddot{D}_{it}, W_{it}] = r_{it,T}$ with $\|r_{it,T}\|_2 \le C/T$, so

$$M(\theta_0, \eta_0) = \mathbb{E}[\tilde{D}_{it} r_{it,T}] \le \|\tilde{D}_{it}\|_2 \, \|r_{it,T}\|_2 = O(T^{-1}),$$

which yields the bias term $O(\sqrt{N}/T)$ in the $\sqrt{N}$-scaled expansion. If $\sqrt{N}/T \to 0$, this term is $o(1)$ and does not affect the limiting distribution in Theorem 1.

A.3 A.1.2 Global within demeaning and fold purity

The blocked-time cross-fitting scheme is designed to prevent nuisance learners from exploiting serial dependence by training on observations too close in time to the held-out block. Global within demeaning couples all time periods through the unit mean $\bar{A}_i = T^{-1}\sum_{t=1}^{T} A_{it}$, so one may worry that it reintroduces train–test dependence. Here we record a simple bound showing that this coupling is weak in large T: each held-out observation enters a training-period within residual only through $\bar{A}_i$ with weight $1/T$, so the induced cross-block correlation vanishes as $T \to \infty$.

A covariance bound. Fix a unit i and write $\bar{U}_i := T^{-1}\sum_{r=1}^{T} U_{ir}$ and $\ddot{U}_{it} := U_{it} - \bar{U}_i$. For any $t, s \in \{1, \dots, T\}$,

$$\begin{aligned}\mathrm{Cov}(\ddot{U}_{it}, U_{is}) &= \mathrm{Cov}(U_{it}, U_{is}) - \mathrm{Cov}(\bar{U}_i, U_{is}) \\ &= \mathrm{Cov}(U_{it}, U_{is}) - \frac{1}{T}\sum_{r=1}^{T} \mathrm{Cov}(U_{ir}, U_{is}).\end{aligned}$$

Under Assumption 2, standard mixing inequalities imply that the autocovariances of (U_{it}) are absolutely summable, so there exists a constant $C < \infty$ (uniform in s and T) such that

$$\left|\sum_{r=1}^{T} \mathrm{Cov}(U_{ir}, U_{is})\right| \le C.$$

Therefore,

$$\left|\mathrm{Cov}(\ddot{U}_{it}, U_{is}) - \mathrm{Cov}(U_{it}, U_{is})\right| \le \frac{C}{T}.$$

In particular, if t is in a training block and s is in a held-out test block separated by at least B_T periods, the original covariance $\mathrm{Cov}(U_{it}, U_{is})$ is small under the mixing condition (and $\alpha(B_T) \to 0$), and the remaining dependence induced by global demeaning is of order $O(1/T)$. In the i.i.d. benchmark (no serial dependence), the formula gives $\mathrm{Cov}(\ddot{U}_{it}, U_{is}) = -\mathrm{Var}(U_{it})/T$ for $t \neq s$.

Implication for the fold-purity discussion. Global within demeaning does create mechanical correlation between training-period within residuals and held-out shocks, but the strength of this correlation vanishes with T. This is why, in the large-T framework used for our asymptotic results, applying the within filter prior to fold construction does not undo the intended time-block separation for nuisance learning. If one nevertheless wants exact fold purity in finite samples, Section 4

describes a fold-specific demeaning variant that computes unit means using only the training periods for each fold.

A.4 A.2 Proof sketch for Theorem 2 (variance consistency)

Write the influence function as $\varphi_{it} = -J_0^{-1}\psi_{it}$ with $\psi_{it} = \psi(\cdot, \theta_0, \eta_0)$. Under the conditions of Theorem 1, a law of large numbers implies $\hat{J} \xrightarrow{p} J_0$. Moreover, cross-fitting plus moment bounds imply that replacing ψ_{it} by $\hat{\psi}_{it}$ is asymptotically negligible in the cluster sums:

$$\sum_{t\in\mathcal{T}_{\text{use}}} \hat{\psi}_{it} = \sum_{t\in\mathcal{T}_{\text{use}}} \psi_{it} + o_p(\sqrt{N}).$$

Define $\Psi_i := \sum_{t\in\mathcal{T}_{\text{use}}} \psi_{it}$ and $\hat{\Psi}_i := \sum_{t\in\mathcal{T}_{\text{use}}} \hat{\psi}_{it}$. By a law of large numbers for independent clusters, $(1/N)\sum_{i=1}^N \hat{\Psi}_i^2 \xrightarrow{p} \mathbb{E}[\Psi_i^2]$. Under Theorem 1, $\mathbb{E}[\Psi_i] = 0$; under Corollary 1, $\mathbb{E}[\Psi_i] = (T - L_*)M(\theta_0, \eta_0) = O(1)$, which does not affect the scaling of $\mathbb{E}[\Psi_i^2]$ and hence does not alter the consistency argument for $\hat{V}$. Note that $S_i = (T - L_*)^{-1}\sum_{t\in\mathcal{T}_{\text{use}}} \varphi_{it} = -J_0^{-1}(T - L_*)^{-1}\Psi_i$, so

$$\text{Var}(\Psi_i) = (T - L_*)^2 J_0^2 \text{Var}(S_i) = (T - L_*)^2 J_0^2 \Omega,$$

where $\Omega = \text{Var}(S_i)$ as in Theorem 1. Since the effective sample size for inference is N (with T entering through within-unit aggregation), and $n = N(T - L_*)$, we have

$$\frac{1}{n^2}\sum_{i=1}^N \hat{\Psi}_i^2 = \frac{1}{N^2(T - L_*)^2}\sum_{i=1}^N \hat{\Psi}_i^2 \xrightarrow{p} \frac{1}{N(T - L_*)^2}\text{Var}(\Psi_i) = \frac{J_0^2}{N}\Omega.$$

Therefore, $\hat{V} = \hat{J}^{-2} \cdot (1/n^2)\sum_{i=1}^N \hat{\Psi}_i^2 \xrightarrow{p} J_0^{-2} \cdot (J_0^2\Omega/N) = \Omega/N$ by Slutsky's theorem.

A.5 A.3 Joint-score extension for (ρ_0, θ_0)

The main text treats inference for θ_0 with the dynamic regressor absorbed into the nuisance set W_{it}. Here we record a joint-score approach for estimating (ρ_0, θ_0) simultaneously.

Let $Z_{it} := (\ddot{Y}_{i,t-1}, \ddot{D}_{it}) \in \mathbb{R}^2$ and define a nuisance regression

$$m_{Z,0}(W_{it}) := \mathbb{E}[Z_{it} \mid W_{it}], \qquad \ell_0(W_{it}) := \mathbb{E}[\ddot{Y}_{it} \mid W_{it}],$$

where now W_{it} may exclude $\ddot{Y}_{i,t-1}$ (e.g., $W_{it} = X_{it}$ or richer lags). Define residuals

$$\tilde{Z}_{it} := Z_{it} - m_{Z,0}(W_{it}), \qquad \tilde{Y}_{it} := \ddot{Y}_{it} - \ell_0(W_{it}).$$

Then the target vector $\beta_0 := (\rho_0, \theta_0)$ solves the orthogonal moment condition

$$\mathbb{E}\Big[\tilde{Z}_{it}\big(\tilde{Y}_{it} - \tilde{Z}_{it}'\beta_0\big)\Big] = 0.$$

With cross-fitted estimates $(\hat{m}_Z, \hat{\ell})$, one obtains the DML estimator

$$\hat{\beta} = \left(\frac{1}{n}\sum \hat{\tilde{Z}}_{it}\hat{\tilde{Z}}_{it}'\right)^{-1}\left(\frac{1}{n}\sum \hat{\tilde{Z}}_{it}\hat{\tilde{Y}}_{it}\right),$$

and inference can proceed using a cluster-robust sandwich variance estimator. The orthogonality logic and product-rate conditions extend to the vector case with standard modifications.

Nickell bias in the joint score. Because Z_{it} contains the within-demeaned lagged outcome $\ddot{Y}_{i,t-1}$, within demeaning typically induces $\mathbb{E}[\ddot{U}_{it} \mid Z_{it}, W_{it}] \neq 0$ in finite samples (Nickell bias). Thus, the joint-score formulation does not make the dynamic regressor exogenous; it only makes the moment condition orthogonal to first-stage (nuisance) estimation error. Allowing W_{it} to exclude $\ddot{Y}_{i,t-1}$ may be convenient for nuisance modeling, but it does not remove the within-induced correlation between $\ddot{Y}_{i,t-1}$ and $\ddot{U}_{it}$.

For $\sqrt{N}$ inference on $\beta_0 = (\rho_0, \theta_0)$ in the large-N, large-T regime, one can impose the vector analogue of Assumption 4: when Z_{it} includes $\ddot{Y}_{i,t-1}$,

$$\mathbb{E}[\ddot{U}_{it} \mid Z_{it}, W_{it}] = r_{it,T} \quad \text{with} \quad \|r_{it,T}\|_2 \leq C/T \quad \text{and} \quad \sqrt{N}/T \to 0.$$

This implies the induced violation of the joint moment condition enters at Nickell order $1/T$ and is $o(N^{-1/2})$, so it is asymptotically negligible for inference (cf. Corollary 1). When T is small, additional bias correction or moment-based dynamic panel methods are needed for reliable inference on ρ_0.

A.6 A.4 Detailed Simulation Results

Table 8 reports detailed simulation results for all scenarios and methods, including bias, RMSE, empirical standard deviation, mean standard error, coverage, and size over $R = 200$ Monte Carlo replications.

A.7 A.5 Simulation Inference Diagnostics

Table 9 reports SE ratios (mean reported SE divided by empirical SD) for the simulation grid.

A.8 A.6 Scaling Experiment: Growing T and Buffers B_T

To better align Monte Carlo evidence with Assumption 1 (where $T \to \infty$ and $B_T \to \infty$ with $B_T/T \to 0$), we run auxiliary experiments that vary T and compare blocked-time DML under buffer rules that grow with T (e.g., $B_T = \lceil \log T \rceil$ and $B_T = \lfloor \sqrt{T} \rfloor$). We report extended diagnostics (bias, RMSE, SD vs. mean SE, t-statistics, and invalid counts) to distinguish bias-driven undercoverage from variance mis-scaling.

Main nonlinear DGP with Lasso.

Table 8: Detailed Monte Carlo results: bias, RMSE, empirical standard deviation (Emp. SD), mean standard error (Mean SE), coverage of 95% confidence intervals, and size (fraction of replications with valid standard errors) over $R = 200$ replications.

Scenario	Method	Bias	RMSE	Emp. SD	Mean SE	Coverage	Size
rho=0.0, p=50, nonlinear	FE-OLS	0.0021	0.0277	0.0277	0.0272	0.945	1.000
rho=0.0, p=50, nonlinear	Post-ML (Lasso)	0.0032	0.0281	0.0280	0.0267	0.935	1.000
rho=0.0, p=50, nonlinear	Orthogonal-no-split (Lasso)	0.0003	0.0278	0.0279	0.0265	0.940	1.000
rho=0.0, p=50, nonlinear	DML (Lasso)	0.0079	0.0300	0.0290	0.0265	0.905	1.000
rho=0.5, p=50, nonlinear	FE-OLS	-0.0093	0.0288	0.0274	0.0272	0.915	1.000
rho=0.5, p=50, nonlinear	Post-ML (Lasso)	-0.0078	0.0286	0.0275	0.0267	0.915	1.000
rho=0.5, p=50, nonlinear	Orthogonal-no-split (Lasso)	-0.0111	0.0297	0.0276	0.0266	0.905	1.000
rho=0.5, p=50, nonlinear	DML (Lasso)	0.0046	0.0298	0.0295	0.0266	0.895	1.000
rho=0.8, p=50, nonlinear	FE-OLS	-0.0041	0.0285	0.0283	0.0275	0.955	1.000
rho=0.8, p=50, nonlinear	Post-ML (Lasso)	-0.0016	0.0288	0.0288	0.0269	0.940	1.000
rho=0.8, p=50, nonlinear	Orthogonal-no-split (Lasso)	-0.0033	0.0286	0.0284	0.0269	0.945	1.000
rho=0.8, p=50, nonlinear	DML (Lasso)	0.0081	0.0316	0.0307	0.0268	0.885	1.000
rho=0.4, p=200, nonlinear	FE-OLS	-0.0117	0.0324	0.0303	0.0291	0.945	1.000
rho=0.4, p=200, nonlinear	Post-ML (Lasso)	0.0212	0.0407	0.0348	0.0258	0.805	1.000
rho=0.4, p=200, nonlinear	Orthogonal-no-split (Lasso)	-0.0283	0.0459	0.0363	0.0263	0.740	1.000
rho=0.4, p=200, nonlinear	DML (Lasso)	0.0147	0.0365	0.0335	0.0268	0.865	1.000
rho=0.4, p=50, linear	FE-OLS	-0.0311	0.0423	0.0288	0.0297	0.800	1.000
rho=0.4, p=50, linear	Post-ML (Lasso)	-0.0324	0.0436	0.0293	0.0282	0.765	1.000
rho=0.4, p=50, linear	Orthogonal-no-split (Lasso)	-0.0319	0.0429	0.0288	0.0292	0.770	1.000
rho=0.4, p=50, linear	DML (Lasso)	-0.0181	0.0348	0.0298	0.0292	0.900	1.000
rho=0.4, p=50, strong confound	FE-OLS	0.0044	0.0226	0.0223	0.0227	0.955	1.000
rho=0.4, p=50, strong confound	Post-ML (Lasso)	0.0092	0.0268	0.0252	0.0218	0.910	1.000
rho=0.4, p=50, strong confound	Orthogonal-no-split (Lasso)	0.0042	0.0227	0.0224	0.0222	0.960	1.000
rho=0.4, p=50, strong confound	DML (Lasso)	0.0116	0.0263	0.0236	0.0220	0.895	1.000

Notes: All methods use unit-clustered robust standard errors. DML uses blocked-time cross-fitting with $K = 4$ folds. Coverage and size marked as "–" indicate standard errors were not available or invalid.

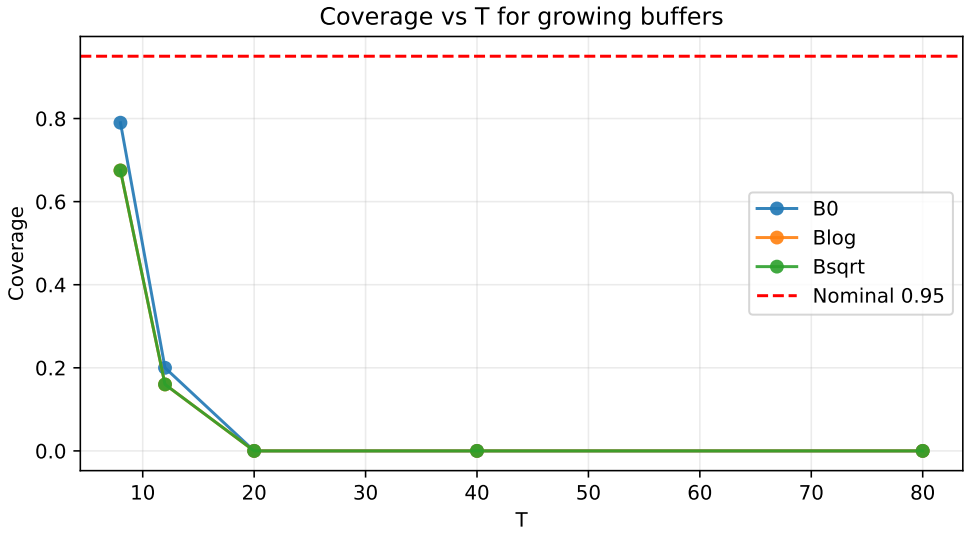

Figure 6: Coverage versus T for growing buffer rules (nonlinear DGP + Lasso).

Table 9: Inference diagnostics: SE ratios (mean reported SE / empirical SD).

Scenario	FE-OLS	Post-ML (Lasso)	Orthogonal-no-split (Lasso)	DML (Lasso)
rho=0.0, p=50, nonlinear	0.98	0.95	0.95	0.91
rho=0.5, p=50, nonlinear	0.99	0.97	0.96	0.90
rho=0.8, p=50, nonlinear	0.97	0.93	0.94	0.88
rho=0.4, p=200, nonlinear	0.96	0.74	0.72	0.80
rho=0.4, p=50, linear	1.03	0.97	1.01	0.98
rho=0.4, p=50, strong confound	1.02	0.86	0.99	0.93

Notes: Entries show the ratio of mean reported standard error to empirical standard deviation across $R = 200$ replications. Ratios less than 1 suggest SE underestimation (a likely driver of undercoverage). Entries marked as "–" indicate standard errors were not available or empirical SD was missing/zero.

Stationary burn-in check (nonlinear DGP + Lasso).

Explosive-regime stress test.

Oracle and OLS baselines (linear DGP).

ElasticNet baseline (nonlinear DGP).

GBM baseline (nonlinear DGP).

Difficulty ladder and N-scaling panel.

Interpreting the linear N-scaling panel. Table 18 shows modest nonzero mean t-statistics at fixed T, especially when T is small and N is large. This is consistent with Nickell-order within-transformation bias of order $1/T$ when lagged outcomes enter the information set, which appears as an $O(\sqrt{N}/T)$ shift in the $\sqrt{N}$ expansion (Corollary 1).

Nonlinear N-scaling (Lasso/GBM).

Interpretation. In the nonlinear DGP with Lasso (Table 10), coverage deteriorates as T grows because bias does not shrink while SEs tighten: by $T \geq 20$ the mean $\hat{\theta}$ is far from θ_0, the mean t-statistic is large, and coverage collapses. This points to nuisance misfit (a linear learner approximating nonlinear confounding), not a variance-scaling bug. The stationary burn-in check (Table 11 and Figure 7) uses a stabilized feedback coefficient to ensure mixing; coverage still declines with T (about 0.77 at $T = 20$, 0.33 at $T = 40$, 0.20 at $T = 80$) despite small bias. In this burn-in design, the SE/SD ratios also fall sharply (e.g., from about 0.86 at $T = 20$ to about 0.57 at $T = 80$), indicating that variance underestimation is an important driver of the undercoverage rather than a transient-initialization artifact. The original feedback design with a long burn-in pushes the process into an explosive regime (Table 12 and Figure 8); we include it only as a stress test illustrating how inference collapses when the DGP violates weak-dependence intuition. The oracle and OLS

Table 10: Scaling experiment (nonlinear DGP + Lasso): extended diagnostics by T and buffer rule.

T	Rule	B	Train share	Mean $\hat{\theta}$	Bias	RMSE	SD	Mean SE	Median SE	SE/SD	Mean CI len	Mean t	Median $\lvert t\rvert$	Frac $\lvert t\rvert > 1.96$	Coverage	Bad $\hat{\theta}$	Bad SE
8	B0	0	0.75	1.02	0.02	0.03	0.02	0.02	0.02	0.88	0.09	0.99	1.08	0.21	0.79	0	0
8	Blog	2 (target 3)	0.36	1.03	0.03	0.04	0.03	0.02	0.02	0.74	0.08	1.23	1.25	0.33	0.68	0	0
8	Bsqrt	2	0.36	1.03	0.03	0.04	0.03	0.02	0.02	0.74	0.08	1.23	1.25	0.33	0.68	0	0
12	B0	0	0.75	1.06	0.06	0.06	0.02	0.02	0.02	0.77	0.07	3.05	2.98	0.80	0.20	0	0
12	Blog	3	0.36	1.06	0.06	0.07	0.03	0.02	0.02	0.70	0.07	3.33	3.20	0.84	0.16	0	0
12	Bsqrt	3	0.36	1.06	0.06	0.07	0.03	0.02	0.02	0.70	0.07	3.33	3.20	0.84	0.16	0	0
20	B0	0	0.75	1.17	0.17	0.17	0.03	0.01	0.01	0.45	0.05	13.87	13.87	1.00	0.00	0	0
20	Blog	3	0.51	1.17	0.17	0.17	0.03	0.01	0.01	0.48	0.05	13.77	13.77	1.00	0.00	0	0
20	Bsqrt	4	0.43	1.17	0.17	0.17	0.03	0.01	0.01	0.49	0.05	13.86	13.80	1.00	0.00	0	0
40	B0	0	0.75	1.15	0.15	0.15	0.02	0.01	0.01	0.41	0.03	19.21	19.44	1.00	0.00	0	0
40	Blog	4	0.60	1.15	0.15	0.15	0.02	0.01	0.01	0.42	0.03	19.24	19.44	1.00	0.00	0	0
40	Bsqrt	6	0.52	1.15	0.15	0.15	0.02	0.01	0.01	0.42	0.03	19.26	19.42	1.00	0.00	0	0
80	B0	0	0.75	2.23	1.23	1.23	0.05	0.09	0.09	1.82	0.37	13.24	13.27	1.00	0.00	0	0
80	Blog	5	0.66	2.25	1.25	1.26	0.05	0.09	0.09	1.77	0.36	13.72	13.70	1.00	0.00	0	0
80	Bsqrt	8	0.60	2.27	1.27	1.27	0.05	0.09	0.09	1.70	0.36	14.09	14.07	1.00	0.00	0	0

Table 11: Scaling experiment with burn-in (nonlinear DGP + Lasso): extended diagnostics by T and buffer rule.

T	Rule	B	Train share	Mean $\hat{\theta}$	Bias	RMSE	SD	Mean SE	Median SE	SE/SD	Mean CI len	Mean t	Median $\lvert t\rvert$	Frac $\lvert t\rvert > 1.96$	Coverage	Bad $\hat{\theta}$	Bad SE
20	B0	0	0.75	1.01	0.01	0.02	0.01	0.01	0.01	0.86	0.05	0.99	1.00	0.23	0.77	0	0
20	Blog	3	0.51	1.01	0.01	0.02	0.01	0.01	0.01	0.86	0.05	1.05	1.00	0.25	0.75	0	0
20	Bsqrt	4	0.43	1.01	0.01	0.02	0.01	0.01	0.01	0.84	0.05	1.07	1.03	0.26	0.74	0	0
40	B0	0	0.75	1.02	0.02	0.02	0.01	0.01	0.01	0.74	0.03	2.42	2.56	0.67	0.33	0	0
40	Blog	4	0.60	1.02	0.02	0.02	0.01	0.01	0.01	0.73	0.03	2.44	2.60	0.67	0.33	0	0
40	Bsqrt	6	0.52	1.02	0.02	0.02	0.01	0.01	0.01	0.72	0.03	2.45	2.56	0.68	0.32	0	0
80	B0	0	0.75	1.02	0.02	0.02	0.01	0.01	0.01	0.57	0.02	3.48	3.27	0.80	0.20	0	0
80	Blog	5	0.66	1.02	0.02	0.02	0.01	0.01	0.01	0.57	0.02	3.48	3.25	0.81	0.19	0	0
80	Bsqrt	8	0.60	1.02	0.02	0.02	0.01	0.01	0.01	0.58	0.02	3.48	3.26	0.80	0.20	0	0

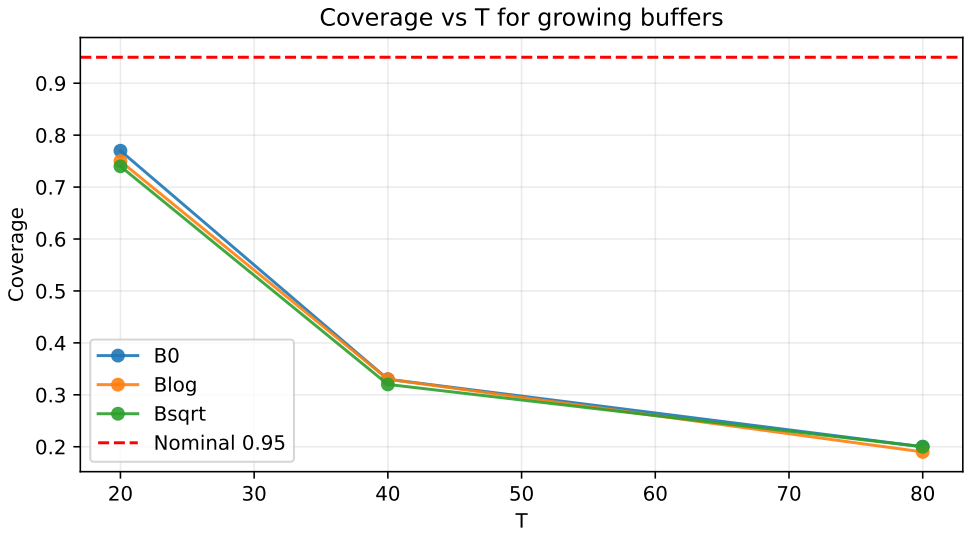

Figure 7: Coverage versus T with a burn-in of 200 periods (nonlinear DGP + Lasso).

Table 12: Burn-in stress test with original feedback (nonlinear DGP + Lasso).

T	Rule	B	Train share	Mean $\hat{\theta}$	Bias	RMSE	SD	Mean SE	Median SE	SE/SD	Mean CI len	Mean t	Median $\lvert t\rvert$	Frac $\lvert t\rvert > 1.96$	Coverage	Bad $\hat{\theta}$	Bad SE
20	B0	0	0.75	3.67	2.67	2.67	0.00	0.00	0.00	0.91	0.00	54748774.46	54731206.53	1.00	0.00	0	0
20	Blog	3	0.51	3.67	2.67	2.67	0.00	0.00	0.00	0.68	0.00	58122220.01	58579741.37	1.00	0.00	0	0
20	Bsqrt	4	0.43	3.67	2.67	2.67	0.00	0.00	0.00	0.60	0.00	60415308.97	60680166.21	1.00	0.00	0	0
40	B0	0	0.75	3.67	2.67	2.67	0.00	0.00	0.00	0.62	0.00	560738032.19	559178540.48	1.00	0.00	0	0
40	Blog	4	0.60	3.67	2.67	2.67	0.00	0.00	0.00	0.54	0.00	576452841.25	570381955.87	1.00	0.00	0	0
40	Bsqrt	6	0.52	3.67	2.67	2.67	0.00	0.00	0.00	0.49	0.00	586296112.36	572855542.40	1.00	0.00	0	0
80	B0	0	0.75	3.67	2.67	2.67	0.00	0.00	0.00	0.94	0.00	32046240240.93	31196343838.51	1.00	0.00	0	0
80	Blog	5	0.66	3.67	2.67	2.67	0.00	0.00	0.00	0.87	0.00	32331645404.44	31483684006.12	1.00	0.00	0	0
80	Bsqrt	8	0.60	3.67	2.67	2.67	0.00	0.00	0.00	0.81	0.00	32506736801.63	31655348614.43	1.00	0.00	0	0

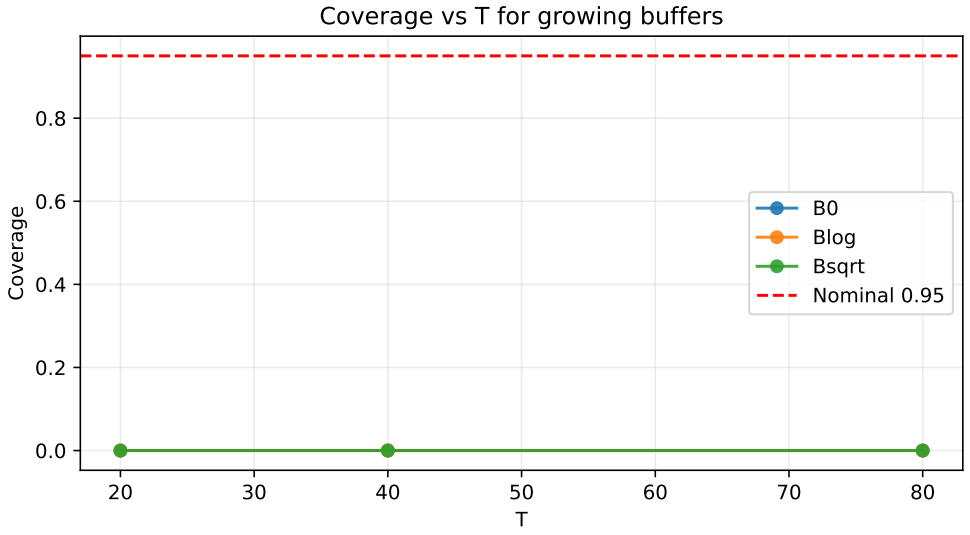

Figure 8: Coverage under a burn-in in the explosive-regime stress test (nonlinear DGP + Lasso).

Table 13: Oracle nuisances (linear DGP): extended diagnostics by T and buffer rule.

T	Rule	B	Train share	Mean $\hat{\theta}$	Bias	RMSE	SD	Mean SE	Median SE	SE/SD	Mean CI len	Mean t	Median $\lvert t\rvert$	Frac $\lvert t\rvert > 1.96$	Coverage	Bad $\hat{\theta}$	Bad SE
8	B0	0	0.75	1.00	-0.00	0.03	0.03	0.03	0.03	0.90	0.11	-0.03	0.71	0.09	0.91	0	0
8	Blog	2 (target 3)	0.36	1.00	-0.00	0.03	0.03	0.03	0.03	0.90	0.11	-0.03	0.71	0.09	0.91	0	0
8	Bsqrt	2	0.36	1.00	-0.00	0.03	0.03	0.03	0.03	0.90	0.11	-0.03	0.71	0.09	0.91	0	0
12	B0	0	0.75	1.00	0.00	0.02	0.02	0.02	0.02	1.07	0.09	0.01	0.62	0.03	0.97	0	0
12	Blog	3	0.36	1.00	0.00	0.02	0.02	0.02	0.02	1.07	0.09	0.01	0.62	0.03	0.97	0	0
12	Bsqrt	3	0.36	1.00	0.00	0.02	0.02	0.02	0.02	1.07	0.09	0.01	0.62	0.03	0.97	0	0
20	B0	0	0.75	1.00	-0.00	0.02	0.02	0.02	0.02	0.98	0.06	-0.02	0.67	0.04	0.96	0	0
20	Blog	3	0.51	1.00	-0.00	0.02	0.02	0.02	0.02	0.98	0.06	-0.02	0.67	0.04	0.96	0	0
20	Bsqrt	4	0.43	1.00	-0.00	0.02	0.02	0.02	0.02	0.98	0.06	-0.02	0.67	0.04	0.96	0	0
40	B0	0	0.75	1.00	-0.00	0.01	0.01	0.01	0.01	0.99	0.04	-0.02	0.71	0.07	0.94	0	0
40	Blog	4	0.60	1.00	-0.00	0.01	0.01	0.01	0.01	0.99	0.04	-0.02	0.71	0.07	0.94	0	0
40	Bsqrt	6	0.52	1.00	-0.00	0.01	0.01	0.01	0.01	0.99	0.04	-0.02	0.71	0.07	0.94	0	0
80	B0	0	0.75	1.00	-0.00	0.01	0.01	0.01	0.01	1.06	0.03	-0.03	0.71	0.04	0.96	0	0
80	Blog	5	0.66	1.00	-0.00	0.01	0.01	0.01	0.01	1.06	0.03	-0.03	0.71	0.04	0.96	0	0
80	Bsqrt	8	0.60	1.00	-0.00	0.01	0.01	0.01	0.01	1.06	0.03	-0.03	0.71	0.04	0.96	0	0

Table 14: OLS nuisances (linear DGP): extended diagnostics by T and buffer rule.

T	Rule	B	Train share	Mean $\hat{\theta}$	Bias	RMSE	SD	Mean SE	Median SE	SE/SD	Mean CI len	Mean t	Median $\lvert t\rvert$	Frac $\lvert t\rvert > 1.96$	Coverage	Bad $\hat{\theta}$	Bad SE
8	B0	0	0.75	0.99	-0.01	0.03	0.03	0.03	0.03	0.94	0.11	-0.43	0.79	0.08	0.92	0	0
8	Blog	2 (target 3)	0.36	0.99	-0.01	0.03	0.03	0.03	0.03	0.88	0.11	-0.42	0.85	0.10	0.91	0	0
8	Bsqrt	2	0.36	0.99	-0.01	0.03	0.03	0.03	0.03	0.88	0.11	-0.42	0.85	0.10	0.91	0	0
12	B0	0	0.75	0.99	-0.01	0.02	0.02	0.02	0.02	0.97	0.09	-0.24	0.72	0.07	0.93	0	0
12	Blog	3	0.36	0.99	-0.01	0.02	0.02	0.02	0.02	0.94	0.09	-0.23	0.69	0.10	0.91	0	0
12	Bsqrt	3	0.36	0.99	-0.01	0.02	0.02	0.02	0.02	0.94	0.09	-0.23	0.69	0.10	0.91	0	0
20	B0	0	0.75	1.00	0.00	0.02	0.02	0.02	0.02	0.95	0.06	0.07	0.67	0.09	0.92	0	0
20	Blog	3	0.51	1.00	0.00	0.02	0.02	0.02	0.02	0.94	0.06	0.07	0.67	0.08	0.92	0	0
20	Bsqrt	4	0.43	1.00	0.00	0.02	0.02	0.02	0.02	0.94	0.06	0.06	0.64	0.09	0.91	0	0
40	B0	0	0.75	1.00	0.00	0.01	0.01	0.01	0.01	0.96	0.04	0.02	0.72	0.07	0.93	0	0
40	Blog	4	0.60	1.00	0.00	0.01	0.01	0.01	0.01	0.96	0.04	0.01	0.72	0.07	0.94	0	0
40	Bsqrt	6	0.52	1.00	0.00	0.01	0.01	0.01	0.01	0.96	0.04	0.01	0.72	0.07	0.94	0	0
80	B0	0	0.75	1.00	-0.00	0.01	0.01	0.01	0.01	1.00	0.03	-0.04	0.68	0.04	0.95	0	0
80	Blog	5	0.66	1.00	-0.00	0.01	0.01	0.01	0.01	1.00	0.03	-0.04	0.69	0.06	0.94	0	0
80	Bsqrt	8	0.60	1.00	-0.00	0.01	0.01	0.01	0.01	1.00	0.03	-0.04	0.69	0.04	0.95	0	0

Table 15: ElasticNetCV nuisances (nonlinear DGP): extended diagnostics by T and buffer rule.

T	Rule	B	Train share	Mean $\hat{\theta}$	Bias	RMSE	SD	Mean SE	Median SE	SE/SD	Mean CI len	Mean t	Median $\lvert t\rvert$	Frac $\lvert t\rvert > 1.96$	Coverage	Bad $\hat{\theta}$	Bad SE
8	B0	0	0.75	1.03	0.03	0.03	0.02	0.02	0.02	0.89	0.08	1.14	1.11	0.19	0.81	0	0
8	Blog	2 (target 3)	0.36	1.03	0.03	0.04	0.03	0.02	0.02	0.80	0.08	1.61	1.54	0.33	0.67	0	0
8	Bsqrt	2	0.36	1.03	0.03	0.04	0.03	0.02	0.02	0.80	0.08	1.61	1.54	0.33	0.67	0	0
12	B0	0	0.75	1.06	0.06	0.06	0.02	0.02	0.02	0.82	0.07	3.02	2.87	0.85	0.15	0	0
12	Blog	3	0.36	1.06	0.06	0.07	0.03	0.02	0.02	0.74	0.07	3.33	3.22	0.87	0.13	0	0
12	Bsqrt	3	0.36	1.06	0.06	0.07	0.03	0.02	0.02	0.74	0.07	3.33	3.22	0.87	0.13	0	0
20	B0	0	0.75	1.18	0.18	0.18	0.03	0.01	0.01	0.42	0.05	13.94	13.84	1.00	0.00	0	0
20	Blog	3	0.51	1.17	0.17	0.17	0.03	0.01	0.01	0.44	0.05	13.86	13.71	1.00	0.00	0	0
20	Bsqrt	4	0.43	1.17	0.17	0.18	0.03	0.01	0.01	0.45	0.05	13.93	13.70	1.00	0.00	0	0
40	B0	0	0.75	1.15	0.15	0.15	0.02	0.01	0.01	0.36	0.03	19.03	19.23	1.00	0.00	0	0
40	Blog	4	0.60	1.15	0.15	0.15	0.02	0.01	0.01	0.36	0.03	19.05	19.25	1.00	0.00	0	0
40	Bsqrt	6	0.52	1.15	0.15	0.15	0.02	0.01	0.01	0.37	0.03	19.07	19.31	1.00	0.00	0	0
80	B0	0	0.75	2.40	1.40	1.41	0.06	0.11	0.11	1.73	0.42	13.30	13.28	1.00	0.00	0	0
80	Blog	5	0.66	2.43	1.43	1.43	0.06	0.10	0.10	1.66	0.41	13.82	13.76	1.00	0.00	0	0
80	Bsqrt	8	0.60	2.45	1.45	1.45	0.06	0.10	0.10	1.59	0.40	14.21	14.12	1.00	0.00	0	0

Table 16: GBM nuisances (nonlinear DGP): extended diagnostics by T and buffer rule.

T	Rule	B	Train share	Mean $\hat{\theta}$	Bias	RMSE	SD	Mean SE	Median SE	SE/SD	Mean CI len	Mean t	Median $\lvert t\rvert$	Frac $\lvert t\rvert > 1.96$	Coverage	Bad $\hat{\theta}$	Bad SE
8	B0	0	0.75	1.26	0.26	0.26	0.05	0.04	0.04	0.91	0.17	6.05	5.99	1.00	0.00	0	0
8	Blog	2 (target 3)	0.36	1.30	0.30	0.31	0.07	0.05	0.05	0.66	0.19	6.36	6.28	1.00	0.00	0	0
8	Bsqrt	2	0.36	1.30	0.30	0.31	0.07	0.05	0.05	0.66	0.19	6.36	6.28	1.00	0.00	0	0
12	B0	0	0.75	1.42	0.42	0.43	0.06	0.09	0.09	1.47	0.36	4.85	4.74	1.00	0.00	0	0
12	Blog	3	0.36	1.46	0.46	0.47	0.08	0.10	0.09	1.19	0.37	5.07	5.01	1.00	0.00	0	0
12	Bsqrt	3	0.36	1.46	0.46	0.47	0.08	0.10	0.09	1.19	0.37	5.07	5.01	1.00	0.00	0	0
20	B0	0	0.75	1.72	0.72	0.72	0.07	0.26	0.25	3.88	1.00	2.88	2.87	0.99	0.01	0	0
20	Blog	3	0.51	1.77	0.77	0.78	0.09	0.25	0.25	2.96	1.00	3.10	3.03	1.00	0.00	0	0
20	Bsqrt	4	0.43	1.77	0.77	0.78	0.10	0.25	0.25	2.57	0.99	3.12	3.07	1.00	0.00	0	0
40	B0	0	0.75	2.20	1.20	1.21	0.07	0.30	0.29	4.36	1.17	4.13	4.16	1.00	0.00	0	0
40	Blog	4	0.60	2.24	1.24	1.24	0.07	0.29	0.29	3.96	1.15	4.32	4.25	1.00	0.00	0	0
40	Bsqrt	6	0.52	2.31	1.31	1.32	0.11	0.27	0.26	2.52	1.05	5.04	4.93	1.00	0.00	0	0
80	B0	0	0.75	3.60	2.60	2.60	0.06	0.01	0.01	0.18	0.04	788.68	345.08	1.00	0.00	0	0
80	Blog	5	0.66	3.61	2.61	2.61	0.05	0.01	0.01	0.19	0.03	694.87	386.33	1.00	0.00	0	0
80	Bsqrt	8	0.60	3.61	2.61	2.61	0.05	0.01	0.01	0.21	0.04	662.40	362.72	1.00	0.00	0	0

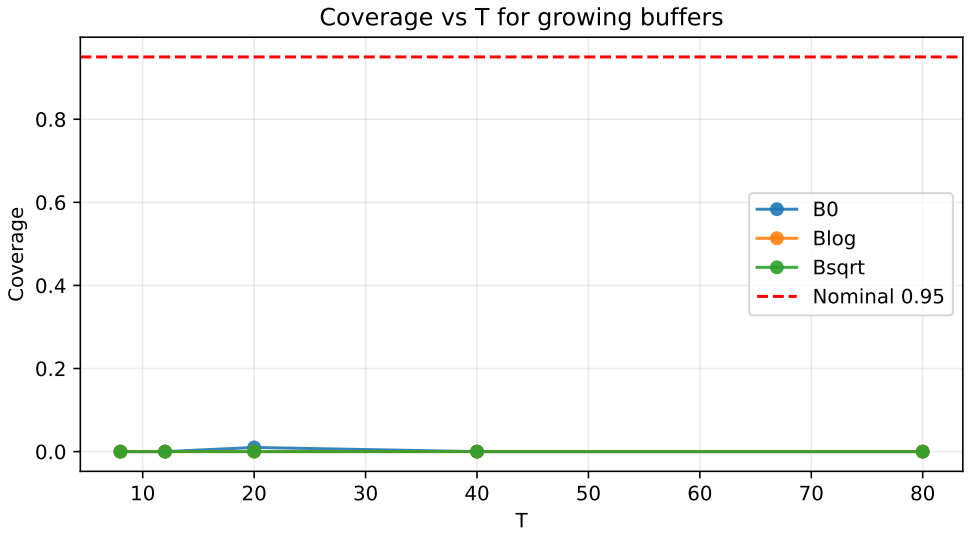

Figure 9: Coverage versus T for growing buffer rules (nonlinear DGP + GBM).

Table 17: Difficulty ladder (nonlinear DGP + Lasso) across $\rho \in \{0.2, 0.5, 0.8\}$ and $\gamma \in \{1, 2\}$.

ρ	γ	T	Rule	B	Train share	Mean $\hat{\theta}$	Bias	RMSE	SD	Mean SE	Median SE	SE/SD	Mean CI len	Mean t	Median $\lvert t\rvert$	Frac $\lvert t\rvert > 1.96$	Coverage	Bad $\hat{\theta}$	Bad SE
0.20	1.00	40	B0	0	0.75	1.02	0.02	0.02	0.01	0.01	0.01	0.78	0.04	1.53	1.54	0.40	0.60	0	0
0.20	2.00	40	B0	0	0.75	1.02	0.02	0.03	0.01	0.01	0.01	0.74	0.03	2.54	2.32	0.65	0.35	0	0
0.50	1.00	40	B0	0	0.75	1.01	0.01	0.02	0.01	0.01	0.01	0.91	0.04	1.37	1.48	0.29	0.71	0	0
0.50	2.00	40	B0	0	0.75	1.02	0.02	0.02	0.01	0.01	0.01	0.72	0.03	2.38	2.53	0.62	0.38	0	0
0.80	1.00	40	B0	0	0.75	1.14	0.14	0.14	0.02	0.01	0.01	0.67	0.04	13.68	13.71	1.00	0.00	0	0
0.80	2.00	40	B0	0	0.75	1.15	0.15	0.15	0.02	0.01	0.01	0.39	0.03	19.47	19.80	1.00	0.00	0	0

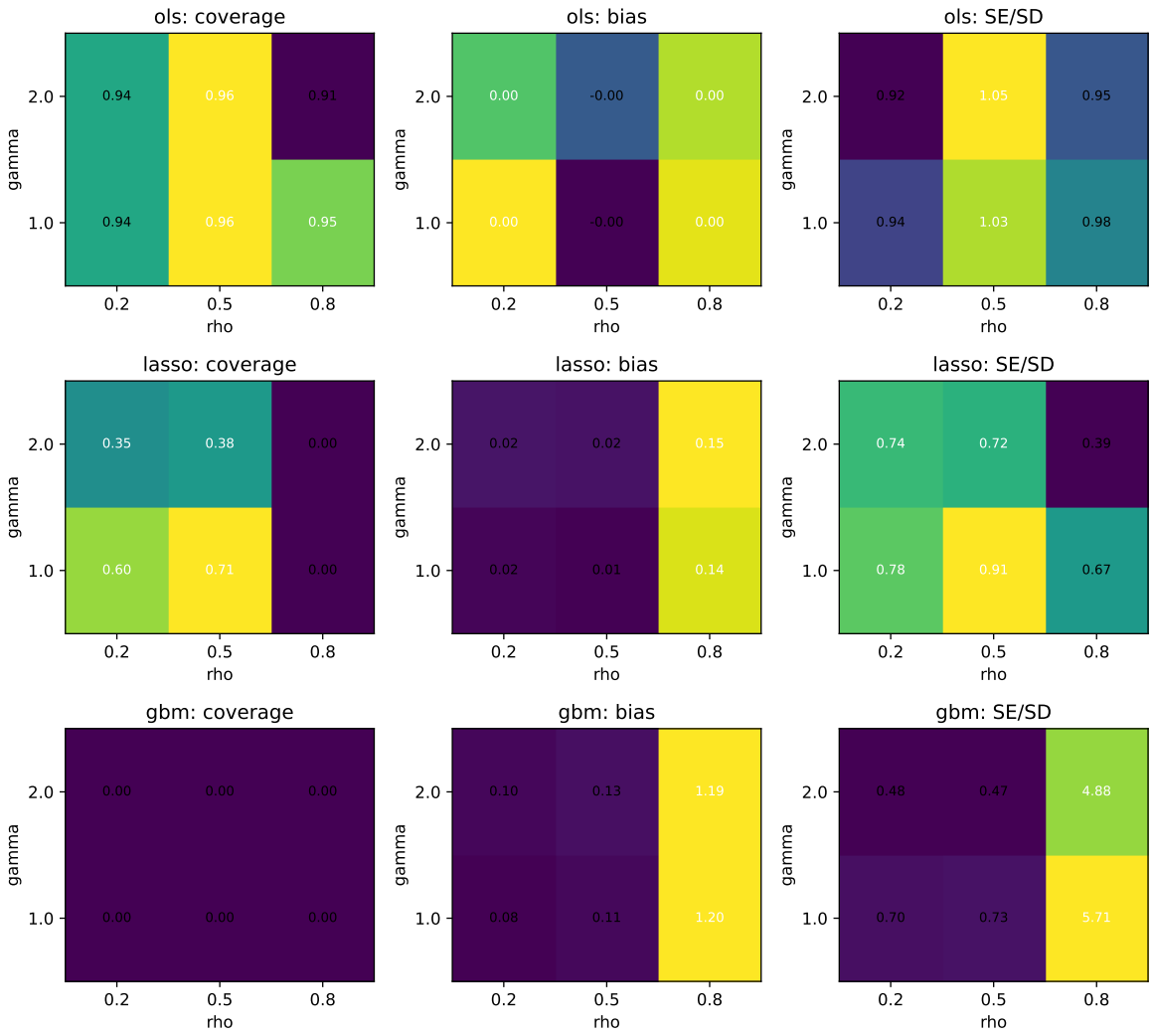

Figure 10: Difficulty ladder at $T = 40$, $B = 0$: coverage, bias, and SE/SD over (ρ, γ) for OLS (linear DGP), Lasso (nonlinear), and GBM (nonlinear).

Table 18: N-scaling panel (linear DGP + OLS) for $N \in \{200, 500, 1000\}$ and $T \in \{20, 40, 80\}$.

N	T	Rule	B	Train share	Mean $\hat{\theta}$	Bias	RMSE	SD	Mean SE	Median SE	SE/SD	Mean CI len	Mean t	Median $\lvert t\rvert$	Frac $\lvert t\rvert > 1.96$	Coverage	Bad $\hat{\theta}$	Bad SE
200	20	B0	0	0.75	1.00	-0.00	0.02	0.02	0.02	0.02	1.03	0.07	-0.23	0.64	0.05	0.95	0	0
200	20	Blog	3	0.51	1.00	-0.00	0.02	0.02	0.02	0.02	1.02	0.07	-0.21	0.65	0.05	0.95	0	0
200	20	Bsqrt	4	0.43	1.00	-0.00	0.02	0.02	0.02	0.02	1.03	0.07	-0.20	0.65	0.06	0.94	0	0
200	40	B0	0	0.75	1.00	-0.00	0.01	0.01	0.01	0.01	0.88	0.04	-0.05	0.88	0.05	0.95	0	0
200	40	Blog	4	0.60	1.00	-0.00	0.01	0.01	0.01	0.01	0.88	0.04	-0.04	0.88	0.05	0.95	0	0
200	40	Bsqrt	6	0.52	1.00	-0.00	0.01	0.01	0.01	0.01	0.88	0.04	-0.04	0.88	0.06	0.94	0	0
200	80	B0	0	0.75	1.00	0.00	0.01	0.01	0.01	0.01	0.95	0.03	0.01	0.69	0.08	0.92	0	0
200	80	Blog	5	0.66	1.00	0.00	0.01	0.01	0.01	0.01	0.96	0.03	0.01	0.71	0.08	0.92	0	0
200	80	Bsqrt	8	0.60	1.00	0.00	0.01	0.01	0.01	0.01	0.96	0.03	0.01	0.71	0.08	0.92	0	0
500	20	B0	0	0.75	1.00	-0.00	0.01	0.01	0.01	0.01	1.00	0.04	-0.30	0.73	0.05	0.95	0	0
500	20	Blog	3	0.51	1.00	-0.00	0.01	0.01	0.01	0.01	0.99	0.04	-0.27	0.74	0.05	0.95	0	0
500	20	Bsqrt	4	0.43	1.00	-0.00	0.01	0.01	0.01	0.01	0.98	0.04	-0.26	0.77	0.05	0.95	0	0
500	40	B0	0	0.75	1.00	-0.00	0.01	0.01	0.01	0.01	1.01	0.03	-0.09	0.56	0.06	0.94	0	0
500	40	Blog	4	0.60	1.00	-0.00	0.01	0.01	0.01	0.01	1.01	0.03	-0.08	0.56	0.07	0.93	0	0
500	40	Bsqrt	6	0.52	1.00	-0.00	0.01	0.01	0.01	0.01	1.01	0.03	-0.08	0.55	0.07	0.93	0	0
500	80	B0	0	0.75	1.00	-0.00	0.00	0.00	0.01	0.01	1.03	0.02	-0.09	0.57	0.07	0.93	0	0
500	80	Blog	5	0.66	1.00	-0.00	0.00	0.00	0.01	0.01	1.03	0.02	-0.09	0.57	0.07	0.93	0	0
500	80	Bsqrt	8	0.60	1.00	-0.00	0.00	0.00	0.01	0.01	1.03	0.02	-0.09	0.56	0.07	0.93	0	0
1000	20	B0	0	0.75	1.00	-0.00	0.01	0.01	0.01	0.01	1.04	0.03	-0.41	0.66	0.09	0.91	0	0
1000	20	Blog	3	0.51	1.00	-0.00	0.01	0.01	0.01	0.01	1.04	0.03	-0.34	0.69	0.09	0.91	0	0
1000	20	Bsqrt	4	0.43	1.00	-0.00	0.01	0.01	0.01	0.01	1.04	0.03	-0.34	0.67	0.09	0.91	0	0
1000	40	B0	0	0.75	1.00	-0.00	0.00	0.00	0.01	0.01	1.15	0.02	-0.37	0.61	0.05	0.95	0	0
1000	40	Blog	4	0.60	1.00	-0.00	0.00	0.00	0.01	0.01	1.14	0.02	-0.36	0.60	0.05	0.95	0	0
1000	40	Bsqrt	6	0.52	1.00	-0.00	0.00	0.00	0.01	0.01	1.14	0.02	-0.35	0.60	0.05	0.95	0	0
1000	80	B0	0	0.75	1.00	0.00	0.00	0.00	0.00	0.00	0.97	0.01	0.07	0.61	0.08	0.92	0	0
1000	80	Blog	5	0.66	1.00	0.00	0.00	0.00	0.00	0.00	0.97	0.01	0.07	0.61	0.08	0.92	0	0
1000	80	Bsqrt	8	0.60	1.00	0.00	0.00	0.00	0.00	0.00	0.97	0.01	0.07	0.61	0.08	0.92	0	0

baselines (Tables 13 and 14) deliver stable SE/SD ratios near one and near-nominal coverage across T and buffer rules, confirming the score and variance normalization. ElasticNet and GBM (Tables 15 and 16) do not mitigate the bias-driven collapse in this high-persistence/high-confounding design; GBM in particular exhibits even larger bias at longer T. Table 16 is run under the same nonlinear high-persistence/high-confounding DGP as the other scaling tables (as opposed to the separate explosive-regime burn-in stress test). The GBM bias ≈ 1.2 cited in the nonlinear N-scaling discussion corresponds to $T = 40$; it increases further to about 2.6 by $T = 80$, with essentially zero coverage. The extreme and non-monotone SE/SD ratios in the GBM table should therefore be read as part of the misspecification/failure-mode narrative: under severe nuisance misfit, the DML linearization and its variance estimator can behave erratically because the cross-fitted residuals and the estimated Jacobian inherit large approximation errors, unlike the oracle/OLS baselines. The difficulty ladder (Table 17 and Figure 10) shows undercoverage worsening with stronger dependence and confounding. The nonlinear N-scaling check (Table 19 and Figure 11) indicates bias is largely flat in N (Lasso bias ≈ 0.15, GBM bias ≈ 1.2) while mean SE shrinks, reinforcing an approximation-driven interpretation.

Table 19: Nonlinear N-scaling at $T = 40$, $B = 0$, $\rho = 0.8$, $\gamma = 2$: bias and coverage by learner.

N	Learner	Mean $\hat{\theta}$	Bias	Mean SE	SE/SD	Coverage
200	gbm	2.20	1.20	0.30	4.22	0.00
500	gbm	2.19	1.19	0.19	3.48	0.00
1000	gbm	2.19	1.19	0.14	3.35	0.00
200	lasso	1.15	0.15	0.01	0.38	0.00
500	lasso	1.15	0.15	0.00	0.27	0.00
1000	lasso	1.15	0.15	0.00	0.18	0.00

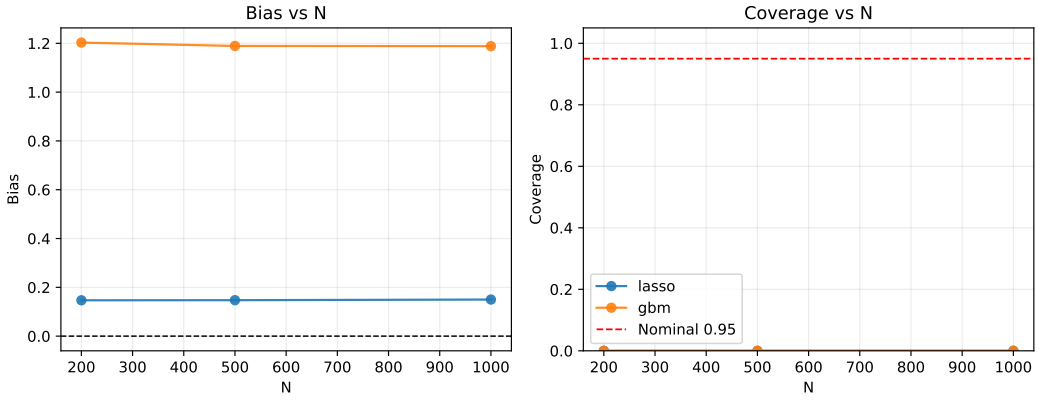

Figure 11: Bias and coverage versus N at $T = 40$, $B = 0$ for Lasso and GBM (nonlinear DGP).